Performance evaluation of new advanced Zr alloys for BWRs and PWRs/VVERs Vol I

Author

Peter Rudling
ANT International, Tollered, Sweden

Technical Contributors

Friedrich Garzarolli
Fürth, Germany

Kit Coleman
Deep River, ON, Canada

Charles Patterson
Clovis, CA, USA

Albert Machiels
Brentwood, CA, USA

Ronald Adamson
Fremont, CA, USA

A.N.T. INTERNATIONAL®

Advanced Nuclear Technology International
Spinnerivägen 1, Mellersta Fabriken plan 4,
448 51 Tollered, Sweden

info@antinternational.com
www.antinternational.com

Ecolabelled printed matter, 4041 0799

Disclaimer

The information presented in this report has been compiled and analysed by Advanced Nuclear Technology International Europe AB (ANT International®) and its subcontractors. ANT International has exercised due diligence in this work, but does not warrant the accuracy or completeness of the information. ANT International does not assume any responsibility for any consequences as a result of the use of the information for any party, except a warranty for reasonable technical skill, which is limited to the amount paid for this report.

Quality-checked and authorized by:

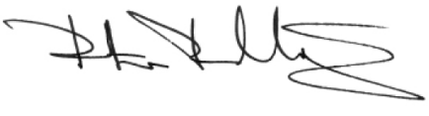

Mr Peter Rudling, President of ANT International

Contents

1 Introduction 1-1

2 Reactor and fuel characteristics 2-1

2.1 General 2-1
2.2 Reactor designs and coolant chemistries 2-3
2.2.1 BWR 2-3
2.2.2 PWR 2-10
2.2.3 VVER 2-15
2.2.4 CANDU 2-17
2.2.5 RBMK 2-22
2.3 Fuel assembly designs 2-22
2.3.1 BWR fuel design 2-22
2.3.2 PWR fuel design 2-24
2.3.3 VVER fuel design 2-25
2.3.4 CANDU fuel design 2-28
2.4 The materials used in fuel assemblies 2-30
2.4.1 Introduction 2-30
2.4.2 Zirconium alloys 2-30
2.4.3 Fuel materials 2-33

3 Irradiation 3-1

3.1 Types of irradiation 3-1
3.2 Effects of irradiation 3-1
3.2.1 Radiolysis 3-1
3.2.2 Effect on Zr alloys 3-8

4 Reactor safety and design criteria related to Zr alloy components 4-1

4.1 Reactor safety 4-1
4.2 Design Criteria related to Normal operation and Anticipated Operational Occurrences (AOO) 4-5
4.2.1 Introduction 4-5
4.2.2 Stress limit during steady state loads 4-5
4.2.3 Creep strain limit during steady state operation 4-5
4.2.4 Maximum strain during power transients, PCI and PCMI 4-9
4.2.5 Maximum stress/strain due to fatigue 4-11
4.2.6 Oxidation, hydriding, CRUD deposition 4-12
4.2.7 Rod internal pressure limit 4-16
4.2.8 Cladding collapse 4-18
4.2.9 Dimensional changes of fuel assembly components 4-19
4.3 Design Criteria related to Design basis accidents 4-30
4.3.1 Seismic event 4-30
4.3.2 LOCA 4-32
4.3.3 RIA 4-36
4.3.4 Dry storage regulations 4-43

5 In-reactor fuel performance (normal operation and AOO) 5-1

5.1 Corrosion and HPU 5-1
5.1.1 Introduction 5-1
5.1.2 Parameters impacting Corrosion and HPU 5-6
5.1.3 BWR Corrosion and HPU 5-16
5.2 Dimensional Changes 5-27
5.2.1 Introduction 5-27
5.2.2 PWR fuel assembly distortion 5-35
5.2.3 Fuel Channel Bowing 5-66
5.3 Mechanical properties 5-69
5.3.1 Introduction 5-69
5.3.2 Unirradiated materials 5-71

5.3.3 Impact of irradiation 5-73
5.4 PCI 5-75
5.4.1 PCI and PCMI 5-75
5.5 Secondary degradation of failed fuel 5-99
5.6 Fatigue 5-101

6 An introduction to Delayed Hydride Cracking (DHC) in zirconium alloys 6-1

6.1.1 Abstract 6-1
6.1.2 Introduction 6-1
6.1.3 Component failure by DHC 6-3
6.1.4 Hydrogen in zirconium 6-13
6.1.5 Basic mechanism of DHC 6-24
6.1.6 Phenomenology 6-26
6.1.7 Models of crack growth rate by DHC 6-38
6.1.8 Assessment – Seven questions 6-45

7 Zr Alloy performance during LOCA and RIA 7-1

7.1 LOCA 7-1
7.1.1 Introduction 7-1
7.2 RIA 7-7
7.2.1 Introduction 7-7
7.2.2 PCMI failure mechanism 7-12

8 Interim dry storage 8-1

8.1 Introduction 8-1
8.2 Degradation Mechanisms 8-1
8.2.1 Air oxidation of cladding 8-1
8.2.2 Thermal Creep 8-2
8.2.3 Stress Corrosion Cracking 8-2
8.2.4 Delayed Hydride Cracking (DHC) 8-2
8.2.5 Hydride reorientation 8-2
8.2.6 Hydrogen migration and redistribution 8-3

References

Unit conversion

1 Introduction

To meet the current situation with more aggressive reactor environments (higher burnups, changing water chemistries and loading patterns), and resolving fuel performance issues such as BWR channel bowing and PWR assembly bowing, a large number of zirconium alloys have been and are being developed. The main driver for the initial material development in Pressurized Water Reactors (PWRs) has been to reduce corrosion rates and Hydrogen Pick-Up Fractions (HPUFs), which have occasionally limited the maximum discharged burnup.

However, to ensure that the new Zirconium Alloys performs satisfactory during normal operation, Anticipated Operational Occurrences (AOOs), postulated accidents and intermediate dry storage, it is crucial to assess the projected performance of components of the new zirconium alloy materials and relate the performance to the material characterises. This assessment is the objective of this Special Topic Report (STR).

This ZIRAT22 STR is an update and expansion of the ZIRAT16 Report since the ZIRAT22 STR also includes BWR material development. However, since the amount of information is so large, this STR is divided into two separate reports, Vol. I (this report) providing the basic information to the detailed material performance in Vol. II. The advantage of this structure is that staff familiar with the basics can only focus on reading Vol. II while staff with less experience can first start to digest the basics in Vol. I before reading Vol. II.

The Report structure is as follows:

- Section 2 provides background information on water reactors and their fuel,
- Section 3 discusses basics of irradiation and impact on water and materials,
- Section 4 gives a backgournd to reactor safety and reviews design criteria related to the Zr alloy components (this means that e.g. fuel melting is not covered here),
- Section 5 presents in-reactor Zr alloy performance during normal operation and anticipated operational occurrences
- Section 6 and 8 contains information about design basis accidents and interim dry storage, respectively

More detailed information of the various topics covered in this report are listed below:

Corrosion and hydriding topics:

- Effects of Coolant Chemistry on Fuel Performance, LCC9 [Rudling et al., 2013]
- LCC7 and 8 STR on PWR/VVER Primary Side Coolant Chemistry Volume I [Riess et al., 2011] and II [Riess& Odar, 2012].
- LCC7 and 8 STR on Introduction to Boiling Water Reactor Chemistry Volume I and II [Cowan et al., 2011 and 2012].
- LCC6 STR on Effect of Zink in BWR and PWR/VVER on Activity Build-up, IGSCC and Fuel Performance [Odar et al., 2010]
- ZIRAT12/IZNA7 STR on Corrosion Mechanisms in Zirconium Alloys[Adamson et al., 2007/2008a].
- LCC2 STR on CRUD in PWR/VVER and BWR Primary Circuits[Riess & Lundgren, 2006].
- ZIRAT8/IZNA3 STR on The Effects of Zn Injection (PWRs and BWRs) and Noble Metal Chemistry (BWRs) on Fuel Performance [Cox et al.,2003/2004].
- ZIRAT9/IZNA4 STR on Corrosion of Zr-Nb Alloys in PWRs[Cox et al., 2004].
- ZIRAT7/IZNA2 STR on Corrosion of Zirconium Alloys[Adamson et al.,2002/2003].
- Water Chemistry and Crud Influence on Cladding Corrosion, ZIRAT6/IZNA1 [Wikmark & Cox, 2001/2002].

- ZIRAT6/IZNA1 STR on CRUD ZIRAT6/IZNA1 STR on Water Chemistry and CRUD Influence on Cladding Corrosion[Wikmark & Cox, 2001].
- Hydriding Mechanisms and Impact on Fuel Performance, ZIRAT5/IZNA1 [Cox & Rudling, 2000].
- Section 6 in ZIRAT/IZNA Annual Reports (ZIRAT5 – ZIRAT21)[Adamsonet al., 2016]
- PWR ZR ALLOY CLADDING WATER SIDE CORROSION (PZAC) [Garzarolli&Garzarolli, 2012]

Thermal and mechanical property topics:

- Processes Going on in Nonfailed Rod During Normal Operation, ZIRAT15/IZNA10 [Patterson & Garzarolli, 2010].
- Processes Going on in Nonfailed Rod During Accident Conditions (LOCA and RIA), ZIRAT15/IZNA10 [Strasser et al., 2010b].
- Pellet Cladding Interaction and Pellet Cladding Mechanical Interaction, ZIRAT11/IZNA6 [Adamson et al., 2006/2007].
- Mechanical Properties of Zirconium Alloys, ZIRAT6/IZNA1 [Adamson & Rudling, 2001/2002].
- MECHANICAL TESTING OF ZIRCONIUM ALLOYS – VOL. I and Vol. II [Adamson et al., 2013 and 2013/2014].

Dimensional changes:

- BWR FUEL CHANNEL DISTORTION [Garzarolli et al., 2011].
- IN-REACTOR CREEP OF ZIRCONIUM ALLOYS [Adamson et al., 2009].
- STRUCTURAL BEHAVIOUR OF FUEL COMPONENTS[Cox et al., 2005/2006].
- DIMENSIONAL STABILITY OF ZIRCONIUM ALLOYS[Adamson & Rudling, 2002/2003].
- IRRADIATION GROWTH OF ZIRCONIUM ALLOYS - A Review (to be published within the ZIRAT22 Programme)

Fuel performance topics:

- Structural Behaviour of Fuel Components, ZIRAT10/IZNA5 [Cox et al., 2005/2006].
- Impact of Irradiation on Material Performance, ZIRAT10/IZNA5 [Adamson & Cox, 2005/2006].
- High Burnup Fuel Issues – Their Most Recent Status, ZIRAT8/IZNA3 [Adamson et al., 2003/2004].
- Dimensional Instability, ZIRAT7/IZNA2 [Adamson & Rudling, 2002/2003].
- HIGH BURNUP FUEL DESIGN ISSUES AND CONSEQUENCES [Rudling et al., 2012].
- IMPACT OF IRRADIATION ON MATERIAL PERFORMANCE [Adamson& Cox, 2005].

Other relevant topics:

- Welding of Zirconium Alloys, ZIRAT12/IZNA7 [Rudling et al., 2007/2008b].
- Manufacturing of Zr-Nb alloys, ZIRAT11/IZNA6 [Nikulina et al., 2006/2007].
- PERFORMANCE EVALUATION OF NEW ADVANCED ZR ALLOYS FOR PWRS/VVERS [Garzarolli &Rudling, 2011].
- PROCESSES GOING ON IN NONFAILED ROD DURING NORMAL OPERATION [Patterson, 2010].

Performance during accident conditions and Interim Dry Storage

- LOSS OF COOLANT ACCIDENTS, LOCA, AND REACTIVITY INITIATED ACCIDENTS, RIA, IN BWRS AND PWRS [Rudling et al., 2004].
- NUCLEAR FUEL BEHAVIOUR UNDER RIA CONDITIONS [Rudling & Jernkvist, 2016].
- DRY STORAGE HANDBOOK [Patterson&Garzarolli, 2015].
- PROCESSES GOING ON IN NONFAILED ROD DURING ACCIDENT Conditions vol II, (ZIRAT15/IZNA10 STR) [Strasser et al., 2010].

2 Reactor and fuel characteristics

2.1 General

There are essentially five different types of commercial water-cooled reactors. By design, the water-cooled reactors in operation can be separated under thermodynamic aspects into Closed Cycle Systems (PWR, VVER, and CANDU) and Open Cycle Systems (BWR and RBMK) [Riess & Millet, 1994].

The separation into “Closed” and “Open Systems” has consequences when it comes to the interaction between radiation and the coolant. In a “Closed” system, the net decomposition of the coolant can be suppressed by the addition of hydrogen or ammonia, whereas in “Open Systems” radiolysis gas is produced and removed from the coolant.

The primary coolant in Closed Cycle System reactors operates under alkaline and reducing conditions with LiOH or KOH as the agents of pH control. This basic principle has been used for more than 30 years and has only been modified within the established framework of specified values for pH control. Such modifications are called “coordinated”, “modified”, “elevated”, or “constant elevated” Li/B-chemistries.

The primary coolant in Open Cycle System reactors has historically operated under neutral and oxygenated conditions while keeping the cycle as clean as possible. However, based on material integrity concerns, the coolant chemistry conditions have been changed in some reactors to reducing conditions (Hydrogen Water Chemistry (HWC), Noble Metal Chemical Addition (NMCA) and Online Noble Chemistry (OLNC).

The fuel in water reactors operates in a wide range of environments. Typical operating conditions for varying reactor types are shown in Table 2-1. Additional information on the thermal-hydraulic conditions in BWR and PWR cores is given in Figure 2-1. For reference, the number and relative generating capacities of each type of operating plant are shown Figure 2-2.

Table 2-1: Design and operating conditions for water cooled reactors.

Parameter		Western type PWR	VVER4 (440/1000) MW	CANDU/ PHWR1	BWR	RBMK2
1.	Coolant	Pressurized H2O	Pressurized H2O	Pressurized D2O	Boiling H2O	Boiling H2O
2.	FuelMaterials (Pressure tube materials)	Zry-4, ZIRLO5, DUPLEX, M5, Inconel, SS3	E110, E635	Zry-4 (Zr2.5Nb)	Zry-2, Zry-4, Inconel, SS	Zr-alloy E110, (Zr2.5Nb)
3.	Average power rating, (MW/m3)	80–125	83/108	9–19	40–57	5
4.	Fast Neutron Flux, Average, n/m².s (E>1MeV)	6–9E17	5-7E17	1.6-4.3E17	4–7E17	1–2E17
5.	Temperatures, °C					
	Average Coolant inlet	279–294	267/290	249–257	200–260 (FW)	270
	Average Coolant outlet	313–329	298/320	293–305	280–288	284
	Max Cladding (outside surface)	320–350	335/352	330	285–305	290
	Steam mass content, %				7–14	14
6.	System pressure, MPa	15.5–15.8	12.5/16.5	10-11	7.0	6.7
7.	Coolant Flow, m/s	3–6*	3.5/6	3–5	2–5*	3.7
8.	Coolant Chemistry**					
	Oxygen, ppb	<5	<10	<10	200-300 (NWC) see also Section 2.2.1	<20
	Hydrogen (D2),					-
	ppm	1.5–4	2.6–5.3	0.3–1	FW (H2) 1-2ppm (HWC without noble metals)	
	cc/kg	17–50	30–60	3 to 10		
					FW (H2) 0.25-0.35ppm (HWC with noble metals)	
	Boron (as H3BO3), ppm	0–2200	0–1500	–***	–	–
	Li (as LiOH), ppm	0.2–6.0	0.05–0.5	0.35-1.4	–	–
	K (as KOH), ppm	–	2–20	–	–	–
	NH3, ppm	–	5–25	–	–	–
	NaOH, ppm	–	0.03–0.35	–	–	–

*Variation from lower to upper part of the core and from plant to plant.
**Zn in ppb quantities may be added for BWRs and PWRs; Pt in ppb quantities may be added for BWRs.
***Not in coolant but in moderator

1. Canadian Deuterium Uranium [CANDU 6 Program Team, 2005]; Pressurised Heavy Water Reactor (PHWR), 2. Reaktor Bolshoi Mozhnosti Kanalov (RBMK), 3. Stainless Steel (SS), 4. Voda Voda Energo Reactor (VVER), 5. Zirconium Low Oxidation (ZIRLO), 6Cladding tube consisting of an outer soft layer and inner layer with high strength - normally high Sn Zry-4

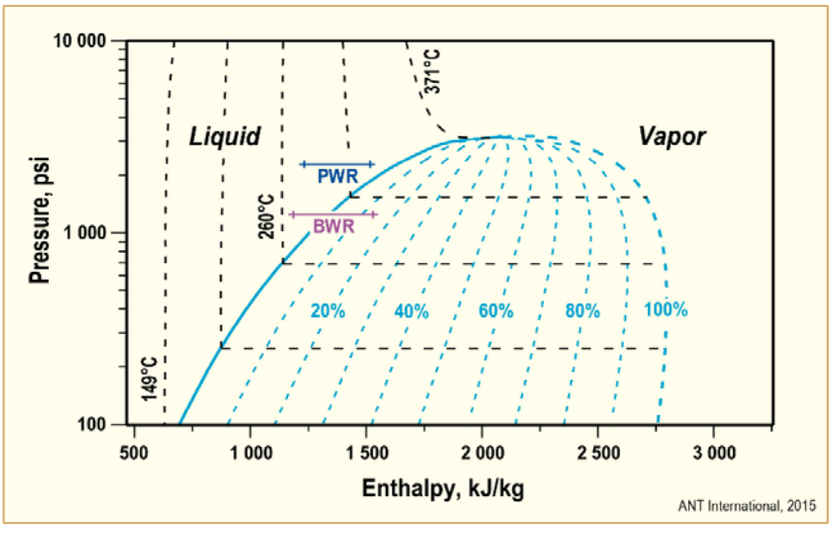

Figure 2-1: Typical thermal-hydraulic conditions in BWRs and PWRs.

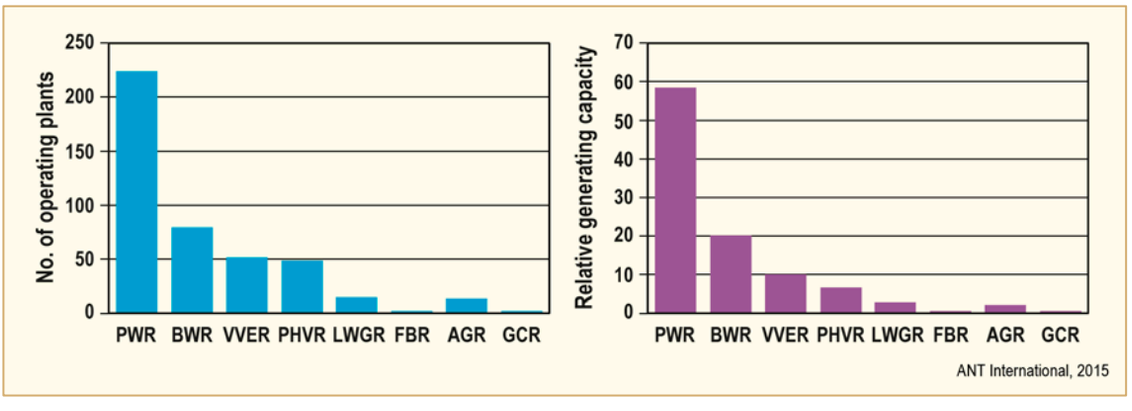

Figure 2-2: Operating power plants, after [IAEA, 2015a].

The reactor types, their characteristics and applied coolant chemistries are described more in the following subsections.

2.2 Reactor designs and coolant chemistries

2.2.1 BWR

One family of BWRsbased on the designs of General Electric (GE) have been constructed in the USA, Japan, Taiwan, Sweden, Spain, Switzerland, Mexico and Germany. A second family of BWRs, the RBMK[1] reactors, were developed in Russia and have been constructed only in countries belonging to the former Soviet Union. This particular BWR design is reviewed in some detail in Section 3.1.4 of FMTR Vol. I, [Cox et al., 2006].

For power plants with BWRs, the main contribution from GE was the reactor or the nuclear island. The Balance of Plant (BOP) was normally constructed by contractors, who specialize on this part of the Nuclear Power Plant (NPP); e.g., turbines, generators, heat exchangers, etc. The reactor design has been changed and improved during the last five decades by GE itself, but additionally by the licence

[1]Reaktor Bolshoi Mozhnosti Kanalov (in English Large Boiling Water Channel).

holders from other countries like Sweden, Japan, Taiwan and Germany. Big changes have been made concerning the recirculation system for the reactor cooling water, the construction materials, the Reactor Water (RW) purification systems, the water separators and steam dryers. The interested reader is referred to LCC7 STR on BWR Reactor Chemistry, Vol. I, [Cowan et al., 2011]. These differences in design can have a significant effect on water chemistry, which is discussed in detail in LCC8 STR on BWR Reactor Chemistry, Vol. II, [Cowan et al., 2012].

As the BOP is often constructed by international companies that normally build fossil-fired power plants, the differences in design of the BOP are much greater than those of the reactor system. However, the designers of the BOP had to keep in mind that the Feed Water (FW) that they supply has a direct influence on corrosion and activity built up in the reactor system.

The BOP is composed of several subsystems. The most important are the FW system, the steam lines, the turbine, and the condensate system. A general overview of a BWR plant is shown in Figure 2-3.

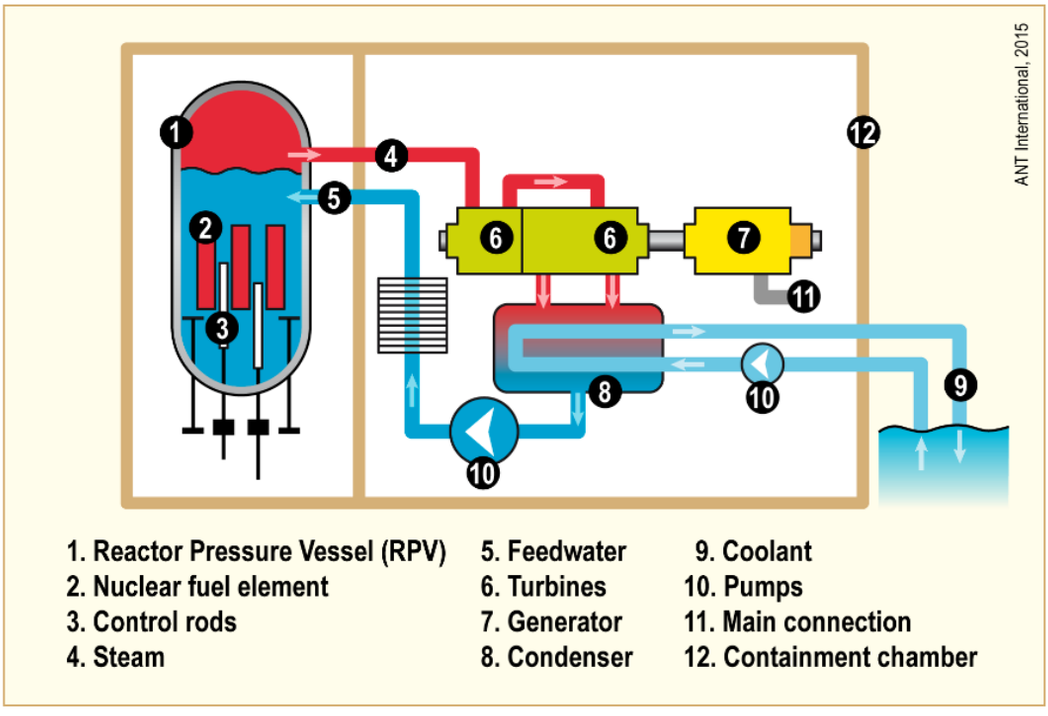

Figure 2-3: Schematic of a BWR, general overview, after [Steffans, 2011].

There are currently 35 BWRs operating in the United States, 24 in Japan, 4 in Taiwan and 2 in Mexico designed by GE, [IAEA, 2014]. In Europe the 14 operating BWRs were designed by:

- GE-H (GE)[2]: Spain 1, Switzerland 2,
- WES AB (ASEA-ATOM): Sweden 7 and Finland 2,
- Areva (Siemens/KWU): Germany 2.

Water chemistry in U.S. and in European BWRs has four common main objectives. These are:

- Ensuring the integrity of the materials against any type of corrosion in all water and steam containing systems and components.
- Minimizing the formation and accumulation of radioactive corrosion products (CPs)

[2] Most of the plants were designed and fabricated before reorganization of the nuclear industry and, for notational convenience, are identified by the names of the respective companies when the plants were developed.

- Ensuring integrity of the fuel.
- Avoiding water ingredients, which are unstable when exposed to radiation, can be activated in the radiation field or are volatile in steam.

During NWC oxidant content (H_2O_2 + O_2) of 125-500 ppb is measured in the reactor coolant in the water sample line before the reactor cleanup system and 20-30 ppm in the steam. These oxidants are formed by radiolysis of the water phase within the core. Because O_2 and H_2 (the other major radiolysis product) are very volatile, during boiling they are stripped to the steam phase, leaving most of the H_2O_2 behind in the water phase. Short lived radical species are also produced in the radiolysis process and they can also affect the oxidizing nature of the coolant e.g. OH, HO_2, O_2^-, and HO_2^-. As calculations indicate in Figure 2-4, both short lived radical species and H_2O_2 may reach quite high concentrations within the fuel element. After traversing the reactor sampling lines, most of the H_2O_2 decomposes on the sample line surface to O_2 and H_2O and the measured H_2O_2 concentration is usually very low [Rooth et al., 1989]. The corrosion potential in water with 300 ppb oxygen would be out-of-pile at 0 to 0.1 V, Standard Hydrogen Electrode (SHE). Within the core of BWRs with NWC even higher values have been found (0.1 to 0.3 V, SHE), which reflects the high red/ox potential of the H_2O_2, [Indig, 1989].

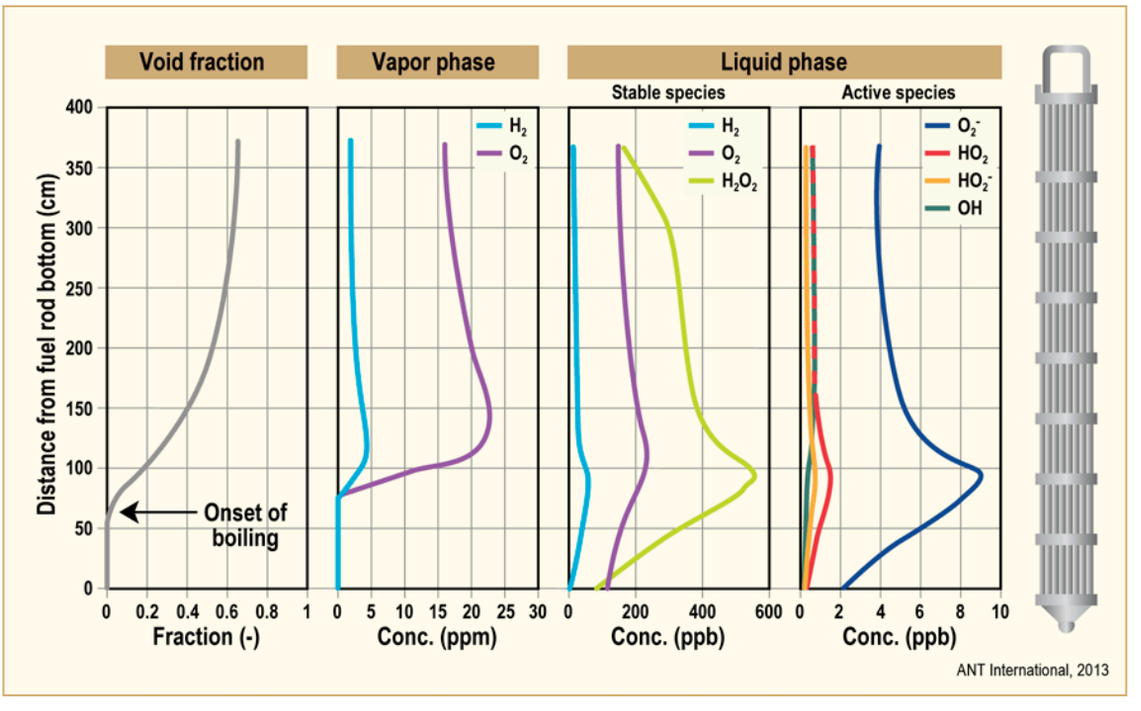

Figure 2-4: Calculated profile of radiolysis species along a fuel rod in a BWR 4 type reactor during NWC, after [Nishino et al., 1998].

Under HWC conditions the radiolytic specie profile changes with increasing feedwater H_2 additions, both inside the fuel channels (Figure 2-5a) and between the fuel channels (Figure 2-5b). H_2 additions cannot suppress radiolytic formation of oxidizing radicals due to the fact that most of the added H_2 is stripped out of the boiling water and into the steam (Figure 2-5a). Electrochemical measurements in BWRs under HWC have shown a significant reduction of the corrosion potential only in the bypass channel whereas in the boiling channel a significant reduction was only seen in the lower, non-boiling sections (Figure 2-5b), [Indig, 1989]. For BWRs utilizing NMCA or OLNC, the conditions inside the fuel channel will be reducing only until the H_2/oxidant ratio is reduced below 2 by boiling. Calculations show that this occurs at an elevation about 60 to 75 cm above the lower end plug.

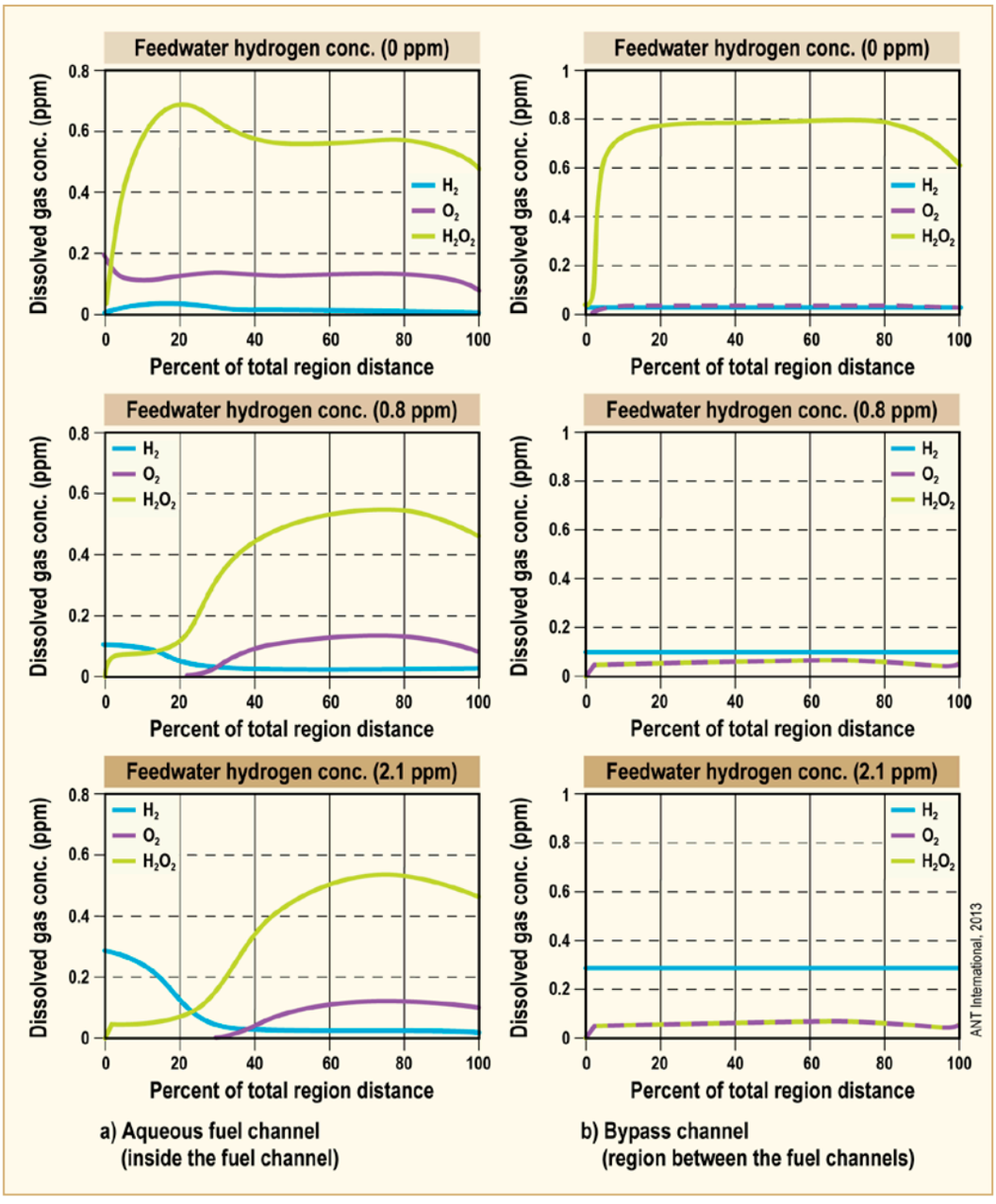

Figure 2-5: Calculated profiles of radiolytic species along a fuel rod in a BWR reactor during HCW for different H additions to the feedwater, after [Ruiz et al., 1989].

The technical approach to water chemistry is different between US and most European BWRs: viz.,

- GE designed plants: HWC (Hydrogen Water Chemistry), Zinc Injection, NMCA/OLNC.
- Siemens and ASEA-ATOM designed plants: NWC

The approaches are driven by the materials of construction, have advantages and disadvantages but lead to similar behaviour of plant materials and comparable fuel reliability.

As there are no indications for sensitization in the core internals of the two German BWRs and as there are no external recirculation loops the “classical” water chemistry has been retained unchanged.

Chemistry issues and areas of concern are similar for all these plants. However, different design and materials concepts favor different chemistry conditions. In particular, the BWRs which are still

3 Irradiation

3.1 Types of irradiation

In reactors the radiation environment consists of neutrons, beta (β), gamma (γ), alpha (α) and fission fragments (Table 3-1).

Neutrons are, of course, the most important form of irradiation. Not only do they allow the reactor to function, they also limit reactor performance due to their effects on corrosion, mechanical properties and dimensional stability.

Fission fragments have high energy and a very short range. They can be propelled from the fuel periphery into the inner surface of the cladding, causing hardening in a depth less than 10 μm, which can be related to microcracks forming there. The other ionizing forms (α, β and γ) cause insignificant irradiation damage compared to neutrons, but have a strong effect on the water radiolysis process, to be discussed in Section 3.2.1, and can increase the electrical conductivity of the normally high-resistance zirconium oxide, Section 3.2.2.4.

Table 3-1: Characteristics of types of radiation [Cox et al., 2006].

Type	Form	Source	Electrical charge	Relative range in metal
neutron	light particle	fission	0	long
alpha (α)	heavy particle	fission radioactive decay	+	very short
beta (β)	very light particle	fission radioactive decay compton effect pair production	-	short
gamma (γ)	wave	fission radioactive decay	0	long
fission fragment	very heavy particle	fission	+, -	very short
				© ANT International,2013

3.2 Effects of irradiation

3.2.1 Radiolysis

Irradiation of water molecules with ionising radiation, primarily γ rays, interact along their pathway and produce ionized and excited water molecules. This leads to the formation of small spherical domains called “spurs” along the pathway of the ionising species where radicals and ionic species are distributed in locally high concentrations (Figure 3-1).

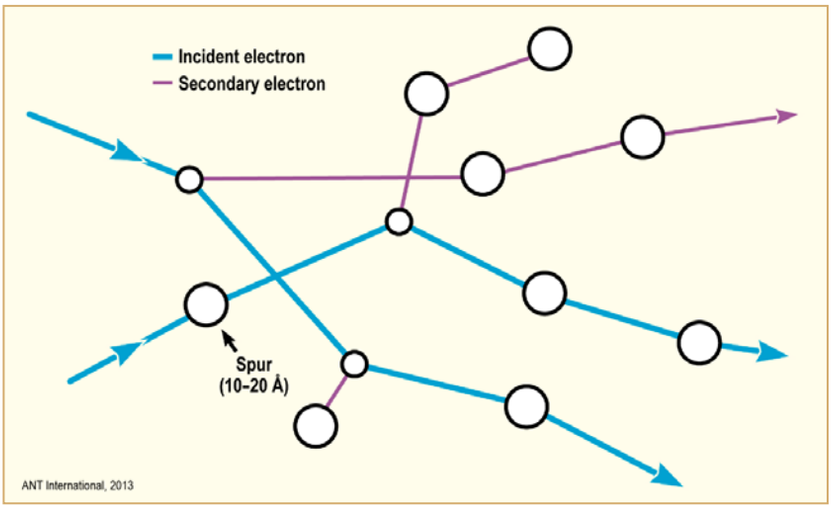

Figure 3-1: Spur formation by high energy electrons, after [IAEA, 1993].

For γ- rays or high energy electrons the primary decomposition products due to the interaction of radiation with the water molecules are:

Equation 3-1: $H_2O \rightarrow e^-_{aq}$, H , OH , H_2, H_2O_2 , HO_2

These active species diffuse and partly react with each other to give some molecular and radical products as shown in Table 3-2.

Table 3-2: Rate Constants of Radiolysis Reactions in Water, after [IAEA, 1993].

Reaction	Rate constant at 25°C $dm^3 \cdot mol^{-1} \cdot sec^{-1}$	Rate constant at 280°C $dm^3 \cdot mol^{-1} \cdot sec^{-1}$
$e^- + H_2O = H^\cdot + OH^\cdot$	1.6 E+1	1.65 E+2
$e^- + H^\cdot = H^\cdot$	2.3 E+10	1.5 E+11
$e^- + OH^\cdot = OH^\cdot$	3.0 E+10	4.05 E+11
$e^- + H_2O_2 = OH^\cdot + OH^\cdot$	1.3 E+10	1.3 E+11
$2H^\cdot = H_2$	2k = 1.0 E+10	1.6 E+11
$e^- + HO_2^\cdot = HO_2^\cdot$	2.0 E+10	2.06 E+11
$e^- + O_2 = O_2^\cdot$	1.9 E+10	2.7 E+11
$2H_2O + 2e^- = H_2 + 2OH^\cdot$	2k = 5.0 E+9	3.0 E+7
$2OH^\cdot = H_2O_2$	2k = 8.4 E+9	8.6 E+10
$OH^\cdot + H^\cdot = e^- + H_2O$	2.0 E+7	6.63 E+8
$H_2O + e^- + H^\cdot = H_2 + OH^\cdot$	2.5 E+10	6.22 E+9
$H_2O + e^- + HO_2^\cdot = OH^\cdot + 2OH^\cdot$	3.5 E+9	8.7 E+8
$H^\cdot + OH^\cdot = H_2O$	2.0 E+10	6.0 E+11
$OH^\cdot + H^\cdot = H^\cdot + H_2O$	4.0 E+7	1.3 E+9
$H^\cdot + H_2O = OH^\cdot = H_2$	1.04 E–4	8.14 E+2
$H^\cdot + O_2 = HO_2$	1.9 E+10	1.96 E+11
$H^\cdot + HO_2^\cdot = H_2O_2$	2.0 E+10	2.06 E+11
$H^\cdot + O_2^\cdot = HO_2^\cdot$	2.0 E+10	2.06 E+11
$H_2O + e^- + O_2^\cdot = HO_2^\cdot + OH^\cdot$	1.3 E+10	1.04 E+10
$H^\cdot + H_2O_2 = OH^\cdot + H_2O$	9.0 E+7	1.2 E+9
$OH^\cdot + H_2O_2 = HO_2^\cdot + H_2O$	3.0 E+7	3.7 E+8
$OH^\cdot + HO_2 = O_2 + H_2O$	1.2 E+10	2.5 E+10
$OH^\cdot + H_2O_2 = HO_2^\cdot + H_2O$	1.8 E+8	5.97 E+9
$HO_2^\cdot + H_2O = OH^\cdot + H_2O_2$	5.7 E+5	1.89 E+7
$H^\cdot + O_2^\cdot = HO_2$	5.0 E+10	5.16 E+11
$HO_2^\cdot + H^\cdot + O_2^\cdot$	8.0 E+5	3.4 E+7
$HO_2^\cdot + O_2^\cdot = O_2 + HO_2^\cdot$	1.5 E+7	4.4 E+8
$2H_2O + 2O_2^\cdot = H_2O_2 + 2OH^\cdot + O_2$	2k = 1.7 E+7	3.27 E+5
$2HO_2^\cdot = H_2O_2 + O_2$	2k = 2.7 E+6	5.2 E+7
$H^\cdot + OH^\cdot = H_2O$	1.4 E+11	1.49 E+12
$H_2O = H^\cdot + OH^\cdot$	2.6 E–5	1.33 E–1
$OH^\cdot + O_2^\cdot = O_2 + OH^\cdot$	1.2 E+10	7.7 E+10
$H_2O_2 = 2OH^\cdot$ (first order, sec^{-1})	2.3 E–12	1.2 E–1
		© ANT International,2013

Only the molecular species have mean lives of more than fractions of a second, Figure 3-2. These ions, radicals and molecular species interact in a series of known reactions, most with low activation energies of ~3 kcal/mole, and in the absence of other added chemical species, form the molecular products H_2, O_2 and H_2O_2 [Burns & Moore, 1976], [Cohen, 1980] and [Lin, 1986]. Nevertheless, the overall stability of water increases with increasing temperature and the yields of molecular decomposition products, H_2, O_2 and H_2O_2, are correspondingly reduced.

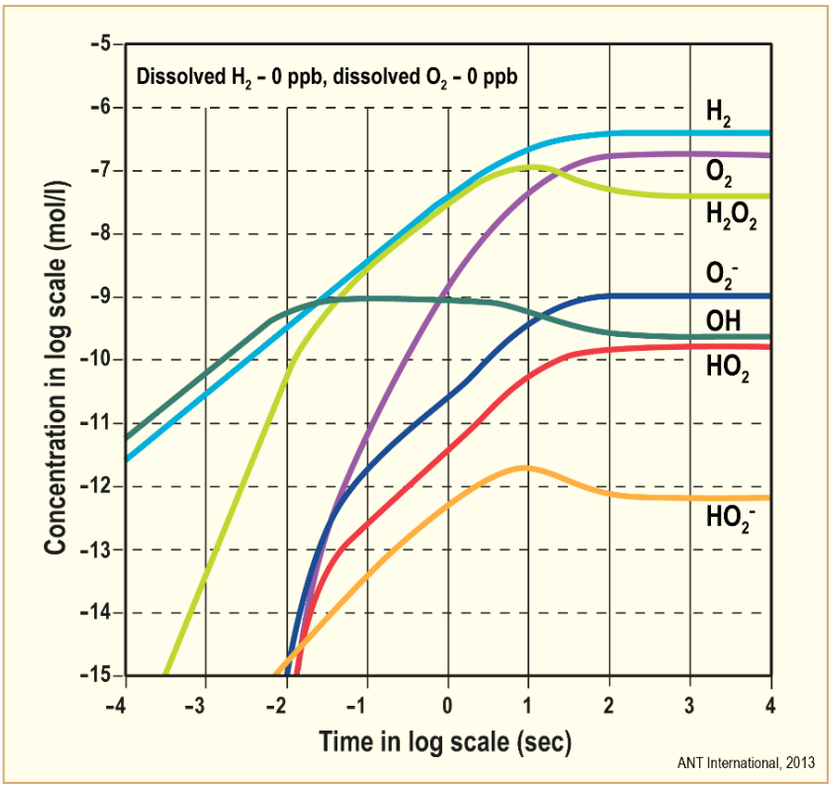

Figure 3-2: Calculated concentrations of radiolytic products in HFIR core at 100W/cc as a function of temperature, after [Jenks, 1965].

The concentrations of the primary products of radiolysis are controlled by the Linear Energy Transfer rate (LET) for each radiation type and energy. The reaction yields are given by so-called G-values, i.e. the number of molecules, ions or radicals formed for each 100 eV of energy absorbed. G-values can vary sharply with the LET so that radiation quality has a significant impact on the primary reaction product concentrations [Cohen, 1980] and [Burns & Moore, 1976]. Typical LET and G-values for neutrons andγ-rays are shown in Table 3-3.

Table 3-3: LET and yields for reactor irradiations, after [Cohen, 1980] and [Burns & Moore, 1976].

Radiation type	Mean LET	G-values: yield/100eV absorbed						
	eV/nm	e^-_{aq}	H^+	H_2O_2	OH·	HO_2·	H·	H_2
β, γ	0.1	2.70	2.70	0.61	2.86	0.03	0.61	0.43
Fast neutrons	40	0.93	0.93	0.99	1.09	0.04	0.50	0.88
© ANT International,2013								

The chemical reactions between the radiolysis products that control the water radiolysis have activation energies of different magnitude. Consequently, the rate of radiolytic reactions and accordingly the yield of radiolysis products change with temperature. The radiolysis modelling calculations indicate the general decrease in radiolytic products with increasing temperature [Jenks, 1965, cited in Cohen, 1969]. This is because, with increasing temperatures, the rate of recombination reactions increases more rapidly than the rate of decomposition reactions [Hisamune et al., 1998]. The temperature dependence of the reaction rate of the fundamental recombination reaction:

Equation 3-2: $OH + H_2 \rightarrow H + H_2O$

is shown in Figure 3-3 as an example [Elliot & Stuart, 2004]. As a consequence, a lower Critical Hydrogen Concentration (CHC) is sufficient to suppress the radiolysis at higher temperatures like PWR operating temperatures, as indicated by Studsvik radiolysis model calculations, Figure 3-4 [Takiguchi et al., 2001], [Sekiguchi & Takiguchi, 1999], and [Meguro, 2008]. Figure 3-4 also shows that the influence of boric acid on CHC is insignificant at temperatures above 150°C.

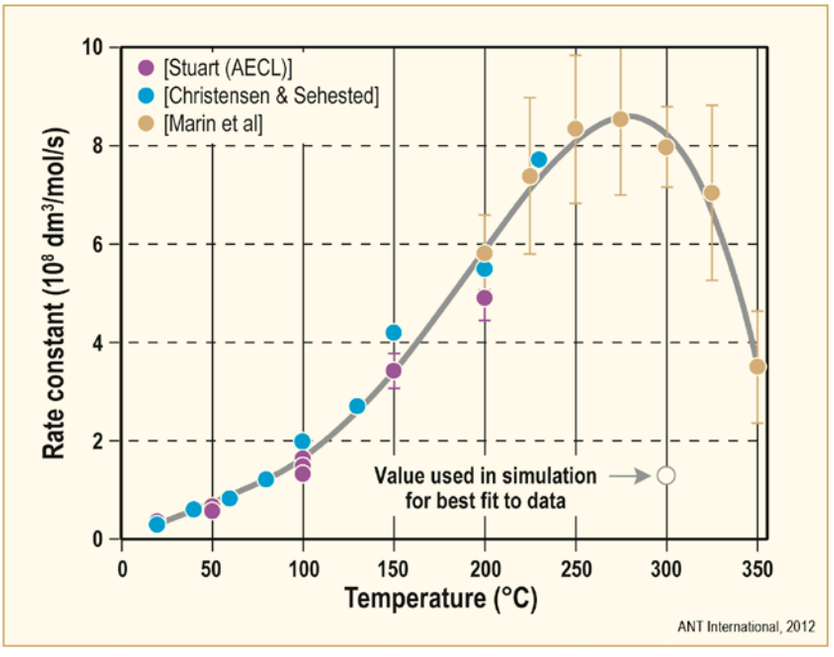

Figure 3-3: Temperature dependence of fundamental recombination reaction of water radiolysis ($OH + H_2 \rightarrow H_2O + H$), after [Elliot & Stuart, 2004].

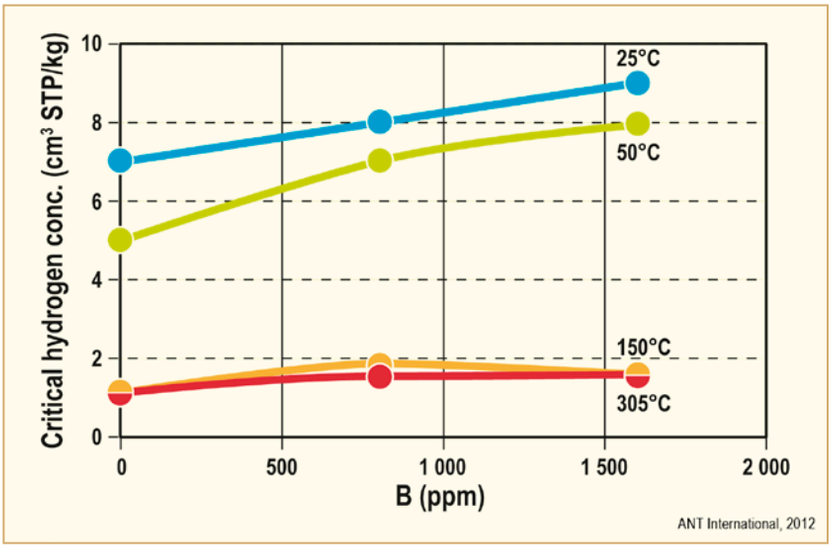

Figure 3-4: Critical hydrogen concentration as a function of temperature calculated by Studsvik radiolysis model, after [Takiguchi et al., 2001] and [Meguro, 2008].

In BWRs with no added hydrogen, i.e. NWC, a significant concentration of non-volatile hydrogen peroxide is formed (along with some hydrogen) some of which then decomposes to oxygen [Lin, 1986], [Ruiz et al., 1989] and [Was & Andresen, 2007]. Although the primary radiolytic decomposition products of water must necessarily eventually produce two molecules of hydrogen for each molecule of oxygen, hydrogen preferentially partitions to the vapour phase in direct cycle BWRs

so that a surplus of oxygen and hydrogen peroxide remain in the aqueous phase. The ~87% of the water that is recirculated in a BWR (since ~11% to 14% of the core flow is transformed into steam) therefore becomes rich in the oxidants O_2 and H_2O_2 [Was & Andresen, 2007]. This leads typically to 20 to 400 ppb dissolved oxygen plus hydrogen peroxide, depending on the precise plant design.

More recently, many BWRs have adopted HWC where about 1 to 2 mg/kg of hydrogen is added to the BWR feedwater, which then mixes with the recirculated water near the top of the annulus (the region of down-flow between the core shroud and pressure vessel). In this way, the concentrations of oxidants, oxygen and hydrogen peroxide, in the aqueous phase are reduced. The efficiency of this recombination process on component surfaces can be significantly improved by the use of noble metal catalyst employed by the NMCA/OLNCtechniques.

The influence of radiolysis on corrosion potentials of core structural materials is also a recurring question. As in all electrochemical corrosion processes, the corrosion potential is a mixed potential arising from the balance of oxidation and reduction reactions occurring on the surface.

The equilibrium potentials of each oxidation or reduction reaction are related to the logarithm of the concentrations of reactants and products via the Nernst equation;

Equation 3-3: $$\varphi = \varphi_0 + RT/nF \cdot \ln([\text{products}]/[\text{reactants}])$$

where $\varphi$is the redox potential, R is the gas constant, T the absolute temperature in K, F is Faraday's constant, and n is the number of electrons involved in the particular electrochemical reaction.

The corrosion potentials of structural metals are principally controlled by the concentrations of molecular oxidants and reductants.

As an example, the Electrochemical Corrosion Potential (ECP) of SS shows a positive potential in normal BWR water chemistry conditions, but a negative one under the same irradiation conditions with (HWC) Figure 3-5.

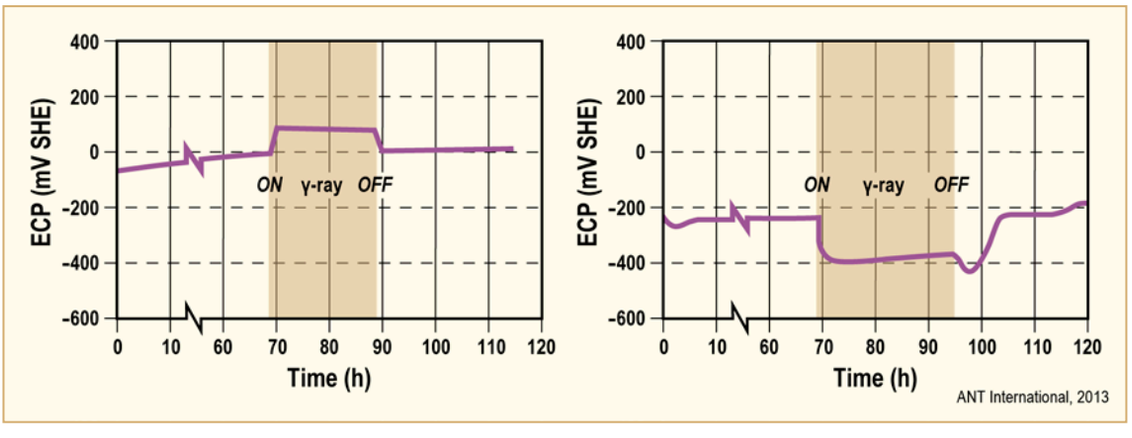

Figure 3-5: Effect of γ-rays on ECP, after [Châtelain et al., 2000].

Similar radiation on/off experiments using irradiated crevices established that no significant change of corrosion potential occurs in irradiated crevices compared to unirradiated conditions, as shown in Figure 3-6. Crevice potentials are always low near the H_2/H_2O redox potential independent of bulk water oxidant concentration [Andresen et al., 1990] and [Was & Andresen, 2007]. This indicates that complete oxidant consumption by corrosion reactions occurs within the occluded volumes of cracks or crevices, independent of the presence or absence of irradiation.

4 Reactor safety and design criteria related to Zr alloy components

4.1 Reactor safety

The requirements for the design of nuclear power plants (including materials for fuel systems) must be evaluated relative to events that are classified with respect to their frequency of occurrence and the severity of their effects on reactor safety. As an example, the regulations in 10 CFR 50.2 define design basis in the U.S. as

> *"…that information which identifies the specific functions to be performed by a structure, system, or component of a facility, and the specific values or ranges of values chosen for controlling parameters as reference bounds for design. These values may be (1) restraints derived from generally accepted "state of the art" practices for achieving functional goals, or (2) requirements derived from analysis (based on calculation and/or experiments) of the effects of a postulated accident for which a structure, system, or component must meet its functional goals."*

The classifications of design events and conditions vary slightly among regulatory authorities and have evolved with experience over the past 10 years, particularly after the earthquake and tsunami that affected the Fukushima Daiichi nuclear power plants in 2011. The classifications are generally based on normal operation (NO), anticipated operational occurrences (AOO), design basis accidents (DBA) and some combination of beyond design basis accidents (BDBA), severe accidents and design extension conditions (DEC). In all countries, the designer/license applicant is expected to identify the specific list of events and faults to be analysed for a given facility, [NEA, 2014].

Typical classifications of design conditions are summarized in Table 4-1. The design conditions of the NRC (10 CFR 50) and the American National Standard ANSI/ANS-57.5 are reflected in the variations developed by many regulatory authorities and are reviewed below. The Standard ANSI/ANS 57.5 was initially approved in 1981, revised in 1996, reaffirmed in 2006 but withdrawn in 2016. The withdrawal is believed to reflect ongoing work to address events represented by what has been identified as Beyond Design Basis Accidents, Severe Accidents or Design Extension Conditions. However, the underlying design condition events of ANSI/ANS-57.5 agree with those of 10 CFR 50 and the IAEA and remain in common usage. The actual ANS standard is, however, unofficial with respect to most regulations.

The frequencies of the design event conditions in Table 4-1 are approximate and are provided for perspective. For example, the bounds for AOOs according to 10 CFR 50 range from once per reactor year to once per reactor life. These limits correspond to a frequency of occurrence less than approximately 0.02 events per reactor year, but are shown as 1 – 0.01 per reactor year in Table 4-1. The frequency ranges in Table 4-1 come from [IAEA, 2016a] and [NEA, 2014].

Table 4-1: Design event conditions and approximate frequencies, [NEA, 2014]

	Normal Operation (NO)	Anticipated Operational Occurrences (AOO)		Design Basis Accidents (DBA)		Beyond Design Basis Accidents (BDBA)	Design Extension Conditions (DEC)
Canada	NO	AOO f > 1E-2/year		DBA 1E-2 > f > 1E-5/year		BDBA f < 1E-5/year	
China	NO	AOO		DBA		Severe Accidents	
Finland	DBC 1	DBC 2 f > 1E-2/year		DBC3 1E-2 > f > 1E-3/year	DBC4 1E-3 > f > 1E-5/year	Severe Accidents f < 1E-5/year	DEC A DEC B
France	PCC 1	PCC2 1 > f > 1E-2/year		PCC3 1E-2 > f > 1E-4/year	PCC4 1E-4 > f > 1E-6/year	Severe Accidents	RRC A RRC B
UK	NO	AOO f > 1E-3/year		DBA f > 1E-5/year		Severe Accidents f < 1E-5/year	Classification up to designer f > 1E-7/year
US (10 CFR 50)	NO	AOO		DBA		Severe Accidents	
US ANSI/ANS-57.5	Condition I	Condition II	Condition III	Condition IV			
DBC = Design Bases Conditions PCC = Plant Condition Category RRC = Risk Reduction Category							
© ANT International 2017							

Conditions of normal operation and operational transients are expected frequently or regularly in the normal course of power operation, manoeuvring, refueling, storage, transport and the storage of fresh and irradiated fuel. These events are identified as Normal Operation or Condition I events. The design requirement for these events is that they shall be "accommodated with margin between any plant parameter and the value of that parameter which would require either automatic or manual protective action", [ANS, 1981].

Anticipated Operational Occurrences (AOOs) are events that can take place at least once in the lifetime of a plant and that have the potential to challenge the safety of the reactor. Generally they have a frequency of occurrence greater than approximately 10^{-2} per reactor-year. AOOs can be subdivided into:

- AOOs of moderate frequency (Condition II events) are those that could occur in a calendar year and that could result in a reactor shutdown. The design requirement for these events is that they shall be accommodated with, at most, a shutdown of the reactor after which the plant can return to power operation after corrective action, but without fuel inspection or repair.

- Infrequent AOOs (Condition **III** events) are incidents that may occur infrequently, if at all, during the life of the plant. The design requirement for these events is that they shall not cause more than a small fraction of the fuel elements in the reactor to be damaged, although sufficient fuel element damage might occur to preclude resumption of operation for a considerable outage time. The resulting release of radioactivity must not be sufficient to interrupt or restrict public use of those areas beyond the plant exclusion area.[24]

Design Basis Accidents (Condition IV events; DBAs) are not expected to occur during the life of a plant, but are postulated and addressed in design and licensing evaluations because the potential consequences include the release of significant amounts of radioactive material. In the ANS/ANS-57.5 standard, Condition IV events represent the limiting design case. The design requirement for these events in the U.S. is that they shall not cause a release of radioactive material that results in an undue risk to public health and safety exceeding the guidelines of 10CFR100. A single Condition IV event shall not cause a consequential loss of system functions needed to cope with the event.

The postulated, maximum credible (single) accident is identified as the design basis accident. For light water reactors, the DBA is generally defined as large-break loss of coolant accident (see 10 CFR 50.46 for example). Accidents that potentially challenge the safety systems of a NPP at a higher level are identified Beyond Design Basis Accidents (BDBA) and may or may not involve core degradation. Similar accidents that lead to significant core degradation are identified as Severe Accidents (SA). The designation Design Extension Conditions (DEC) has been introduced to encompass both types of events and is advocated by some regulators; cf. [IAEA, 2016a] and [IAEA, 2016b]. This set of accidents typically involve the failure of multiple systems that lead to heat removal issues, reactivity excursions or combinations of both and that have the potential for damaging the primary pressure barrier and containment integrity.

The objectives of the *fuel system*[25] safety review is to provide assurance that:

1. The *fuel system* is *not damaged*[26] as a result of normal operation and AOOs.
2. *Fuel system* damage is never so severe as to prevent control rod insertion when it is required.
3. The number of *fuel rod failures*[27] is not underestimated for postulated accidents.
4. *Coolability*[28] is always maintained.

[24] An exclusion area is typically established around each NPP of such size that an the total radiation dose to anyone on the boundary is no greater than a specified set of values over a given time - See Section 100.11 of Title 10 of the Code of Federal Regulations for an example of conditions in the U.S.

[25] Fuel system consists of assemblies of fuel rods including fuel pellets, insulator pellets, springs, tubular cladding, end closures, hydrogen getters, and fill gas; burnable poison rods including components similar to those in fuel rods; holddown spring, connections, spacer grids and springs; end plates; channel boxes; and reactivity control elements that extend from the coupling interface of the control rod drive mechanism in the core.

[26] Not damaged means not only that the fuel integrity is maintained, i.e., no release of radioactivity, but also that the fuel system dimensions remain within operational tolerances, and that functional capabilities are not reduced below those assumed in the safety analysis. This objective implements GDC10 and the design limits that accomplish this are called SAFDLs.

[27] Fuel rod failure means that the fuel cladding has been breached and radioactivity from the fuel get access to the coolant.

[28] Coolability means that the FA retains its rod-bundle geometry with adequate coolant to permit removal of residual heat even after a severe accident.

Objective (1) in the above list is formalized in General Design Criterion 10, GDC10 [10 CFR Part 50 Appendix A, 1990]. The application of *GDC10* is described in the SRP [USNRC, 1981]. The *fuel system*[29], nuclear, and thermal and hydraulic designs are covered in SRP sections 4.2, 4.3 and 4.4, respectively. Section 4.2 in SRP identifies a number of *fuel system* failure mechanisms that actually have occurred in commercial reactors, as well as hypothesized *fuel system* failure mechanisms. For each of these *fuel system* failure mechanisms, SRP section 4.2 lists a corresponding design limit intended to accomplish objective (1) in the list above. These design limits are called SAFDLs. Thus, the SRP does not include any design limits to address potential new *fuel system* failure mechanisms related to more recent fuel designs and/or reactor operation strategies.

Fuel rod failures must be accounted for in the dose analysis required by [10 CFR Part 100], for postulated accidents.

The general requirements to maintain control rod insertability and core coolability appear in the General Design Criteria, e.g., GDC 27 and GDC 35. Specific coolability requirements for the loss of coolant accidents, LOCA, are provided in 10 CFR Part 50 [10 CFR Part 50, §50.46, 1990].

The *fuel system* design bases must take the four objectives described on the previous page into account. The SAFDLs discussed below do this. In a few cases the SAFDLs provide the design limit but in most cases it is up to the fuel vendor to recommend a design limit value, taking a specific failure mechanism into account. The fuel vendor must also provide the background data for the design limits (that are specified by the NRC as well as those used by the specific fuel vendor) to ensure that the design limit is both necessary and sufficient. The fuel vendor must also provide data for the specific fuel design that shows that the design limit is met to get their fuel licensed.

Specific failure mechanisms for the fuel system (including the fuel rod) and licensing criteria related to classes I and II operation and classes III and IV events are and discussed in the following subsections.

The overall objective of reactor safety is the prevention of radiation-related damage to the public from the operation of commercial nuclear reactors.

To meet this objective safety criteria are introduced to avoid fuel failures during normal operation, or to mitigate the consequences from reactor accidents in which substantial damage is done to the reactor core. The current safety criteria were developed during the late 60s and early 70s. The main objective of 10CFR[30]50 and 10CFR100 is to limit radioactive impact on the environment:

- In 10CFR50, the General Design Criterias (GDCs) are specified and interpreted in the Standard Review Plan, SRP, which imposes mechanical, nuclear and thermal hydraulic fuel design criteria that the fuel vendor and the utility must meet.
- In 10CFR100, it is specified that conservative dose calculations must be done to assess the potential impact on the environment during a DBA.

This is handled differently in various countries.

In USA it must be assumed that 100% of the core is failed (even if that is not the case) during a – Large Break Loss of Coolant Accident (LBLOCA) and the calculated dose to the environment must be below the 10CFR100 dose limit, [Shoop, 2004]. The dose calculations for all the other DBAs are calculated based upon the results of the DBA analysis. For RIA, a conservative assumption is used that all rods which experienced a surface heat flux in excess of the DNBR (in PWRs) and CPR (in BWRs) have failed. For the dose calculations, only the source term generated by these assumed failed rods need to be taken into account. Historically, the Nuclear Regulatory Commission (NRC) has defined that during a RIA, the dose must be ≤ 25% of the 10CFR100 dose limits. For other DBAs (other than LBLOCA and RIA), NRC has licensed plants to specific requirements, normally ≤ 10% of the

[29]Fuel system consists of assemblies of fuel rods including fuel pellets, insulator pellets, springs, tubular cladding, end closures, hydrogen getters, and fill gas; burnable poison rods including components similar to those in fuel rods; holddown spring, connections, spacer grids and springs; end plates; channel boxes; and reactivity control elements that extend from the coupling interface of the control rod drive mechanism in the core.

[30]Code of Federal Regulations

10CFR100 limits. The reasons for the difference in maximum allowable dose for different DBAs is that in the case of a LOCA, for example, there is some delay in the radioactivity leaking out to the environment while for other accidents, such as steam generator tube rupture (with lower maximum allowable doses), there is a direct path of the radioactivity to the environment.

In Sweden, dose calculations are not done for LBLOCA since all Swedish nuclear power plants are equipped with a filter that essentially eliminates any spread of activity to the environment during these types of accidents. Also in France, these type of dose calculations are not performed. In Germany, code calculations must show, that less than 10% of the fuel has failed during a LOCA. However, even though the calculated number of failed rods is less than 10%, the 10% number must be used in the dose calculations to be conservative.

4.2 Design Criteria related to Normal operation and Anticipated Operational Occurrences (AOO)

4.2.1 Introduction

This section describes the design criteria related to the fuel components, performance issues and margins towards each criteria with increasing burnup.

4.2.2 Stress limit during steady state loads

Design criterion – Plastic deformation (excluding creep) is regarded as material failure according to the ASME Code, and must therefore not occur. Thus, the maximum stress must be below yield strength.

The stress calculations should assume maximum fretting depth and wall thickness reduction corresponding to maximum oxide thickness. According to the [ASME Code, 2015], the maximum stress level depends on what types of stresses are involved.

Performance Issues – No fuel performance issue has been reported related to the fulfilment of the maximum allowable stress (during non-transient loading) fuel design criterion. With the incorporation of finite element methods in the design of fuel rods and fuel assembly components, procedures of Section III of the ASME pressure vessel code are being replaced by detailed estimates of local stress and strain.

Fresh fuel has the smallest margin towards plastic deformation (yielding) in Zr alloys since the yield strength of the Zr alloy is smallest at start of the irradiation of the fresh fuel and the strength increases and saturates after a few months of irradiation – see Section 5.3.3.

4.2.3 Creep strain limit during steady state operation

Design criterion – For BWR fuel rods a maximum allowable equivalent plastic creep strain of 2.5%, corresponding to about 1.5% plastic tangential strain, is sometimes used by fuel vendors (in Germany and Sweden), see Section 5.2.1.1. The initial creep down of the cladding due to larger system than rod internal pressure is not taken into account. Only the outward creep strain after pellet/cladding contact has occurred is compared to the limit. This outward creep is due to pellet swelling during irradiation and occurs at a very slow rate.

For PWRs a maximum allowable creep strain corresponding to a 1% increase in fuel rod diameter compared to the initial diameter is often used (for example, in Sweden, France, the Netherlands, and Switzerland). This limit is related to the risk of getting DNB if the diameter increase becomes too large to permit the coolant to effectively remove heat from the fuel rod; i.e., a small change comes from $CHF \propto (D_{rod})^{-0.5}$, so that a 1% increase in diameter corresponds to about a 0.5% decrease in CHF, while larger changes are postulated to result from cladding deformation due to lift-off, disruption of heat transfer and the propagation of DNB and lift-off conditions among adjacent fuel rods.

Performance Issues – No issues related to outward creep due to pellet swelling has been reported and it is expected that this will not be the case since in-reactor creep tests have shown that the creep ductility, i.e., the amount of creep strain to failure, is much larger than the maximum limits specified by the fuel design criterion. Below, fuel clad creep data vs. Burnup is provided. In one of the tests, Zry-2 cladding tubes in SRA condition where internally pressurised and irradiated in the PLUTO research reactor in Harwell [Wood, 1974]. The fast flux was 3-4*10^{13} n/cm^2*s (E>1MeV) and the maximum fluence varied between 5-16*10^{20} n/cm^2 (E>1MeV). The creep deformation was measured on-line continuously during irradiation (Figure 4-1). It is clear that in neither case, tertiary creep stage was not reached in any of the tests samples. Maximum creep strain was measured in hot-cell were 3.7, 4.0, 5.7 and 9.7%.

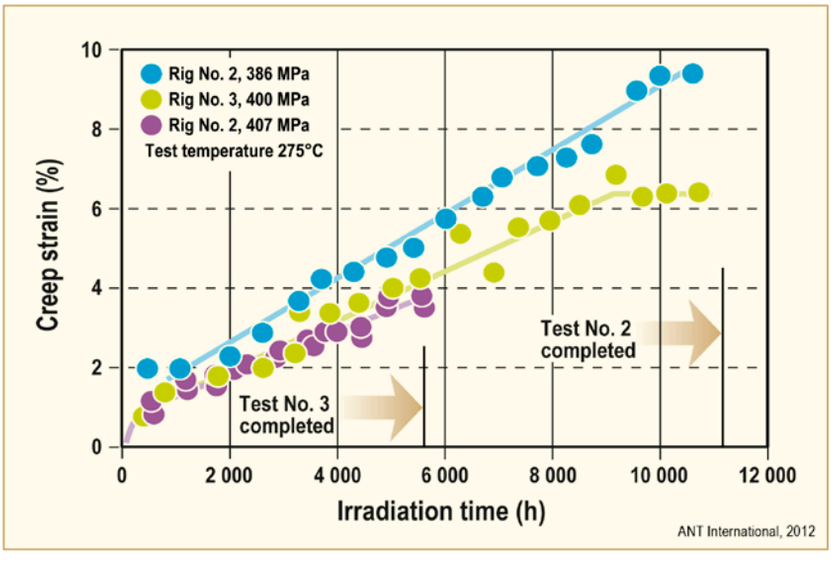

Figure 4-1: Irradiation creep at a temperature of 275°C for SRA Zry-2 tube pressurised in the rig No. 2 and 3 of PLUTO – reactor, after [Wood, 1974].

The pellet swelling will cause fuel cladding outwards creep after pellet/cladding contact has been established.

Irradiation creep data has been obtained to moderate burnup. The highest data is for a test reactor program on Zr2.5Nb to 1.5 x 10^{26} n/m^2 (E> 1MeV) equivalent to a LWR burnup of about 75 MWd/kgU [Causey et al., 2000]. Another extensive test reactor program on Zircaloy-4 and M5 was reported to 7 x 10^{25} n/m^2 (E> 1 MeV) [Soniak et al., 2002]. Commercial reactor data is reported to about 60 MWd/kgU (1.2 x 10^{26} n/m^2 (E> 1 MeV) [Kido et al., 2002]. None of the data raised concerns relative to high burnup creep performance of zirconium alloys.

The creep behaviour of NDA was reported by [Sasakawa et al., 2005] and is shown in (Figure 4-2). The figure shows a maximum diameter decrease of 1.6% at a burnup of 24 MWd/kgU (~4.2E21 n/cm^2) after which the pellet swelling forces the fuel cladding outwards. However, even at maximum burnup, the maximum outward creep is still below the initial diameter.

5 In-reactor fuel performance (normal operation and AOO)

5.1 Corrosion and HPU

This topic is covered extensively in the associated ZIRAT22 Special Topic Report Performance evaluation of new advanced Zr alloys for BWRs and PWRs/VVERs-Vol II [Rudling, 2017] and therefore only briefly discussed in this volume.

5.1.1 Introduction

Corrosion of zirconium alloys is a thermodynamic and electrochemically based process affected by the following parameters, see Figure 5-1:

- The microstructure of the Zr alloy-metal surface.
- The water chemistry and the hydraulic conditions.
- The Zr alloy temperature (at the metal/oxide interface).

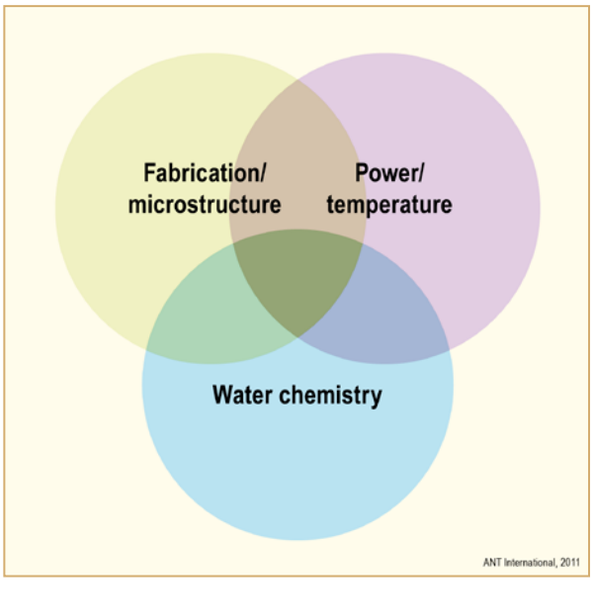

Figure 5-1: Parameters impacting corrosion performance of Zr Alloys.

During the initial oxidation/corrosion of zirconium alloys, a thin protective black oxide is formed. As the zirconium oxide grows in thickness the outer part of the oxide (facing the water/steam phase) is transformed into a greyish porous oxide. The oxide grows inwards into the zirconium alloy material.

In general there exists common understanding that only atomic hydrogen that is generated by cladding corrosion is picked-up by Zr alloys and not the dissolved molecular hydrogen that is added into the reactor coolant. In high temperature water Zr-based alloys build a thin, compact, black protective layer by early oxidation phase with water. Electrons released from Zr by oxidation are captured by hydrogen ions of the water that reduce them to hydrogen atoms. Some of these hydrogen atoms recombine to H_2 molecules and release from the Zr surface as hydrogen gas, whereas the other part can migrate into Zr matrix as soluble H atoms. When the solubility limit for picked-up hydrogen (about 100 mg/kg at 330°C) exceeds in the Zr-alloy, the excess hydrogen precipitates as Zr-Hydride. The ratio of the portion that is picked-up in the Zr alloy to total hydrogen formed by Zr oxidation (corrosion) is defined as Hydrogen Pick-Up Fraction (HPUF). This HPUF, depends on zirconium alloying content but also on temperature, water chemistry, and reactor start-up procedure. The total

amount of hydrogen that is picked up by the Zirconium alloy, HPU is the product of the corrosion rate and the HPUF.

Enhanced Hydrogen Pickup (HPU) in the zirconium (Zr) alloy fuel cladding is one of the largest concerns regarding fuel cladding performance. This is because increased HPU could lead to

- Formation of dense hydride rim, which results in early increase in cladding corrosion (hydride rim corrodes faster than the Zr alloys) during normal reactor operation.
- Increased dimensional changes of Zr alloy fuel assembly components (Hydride has a 15% higher specific volume relative to the metallic Zr).
- Enhanced embrittlement of the Zr alloy components during accident conditions (LOCA, RIA and cask drop accident during interim dry storage (Zr-hydride is hard and brittle) [Garzarolli & Sabol, 2006].

The corrosion and hydriding process of Zirconium alloys is schematically shown in Figure 5-2.

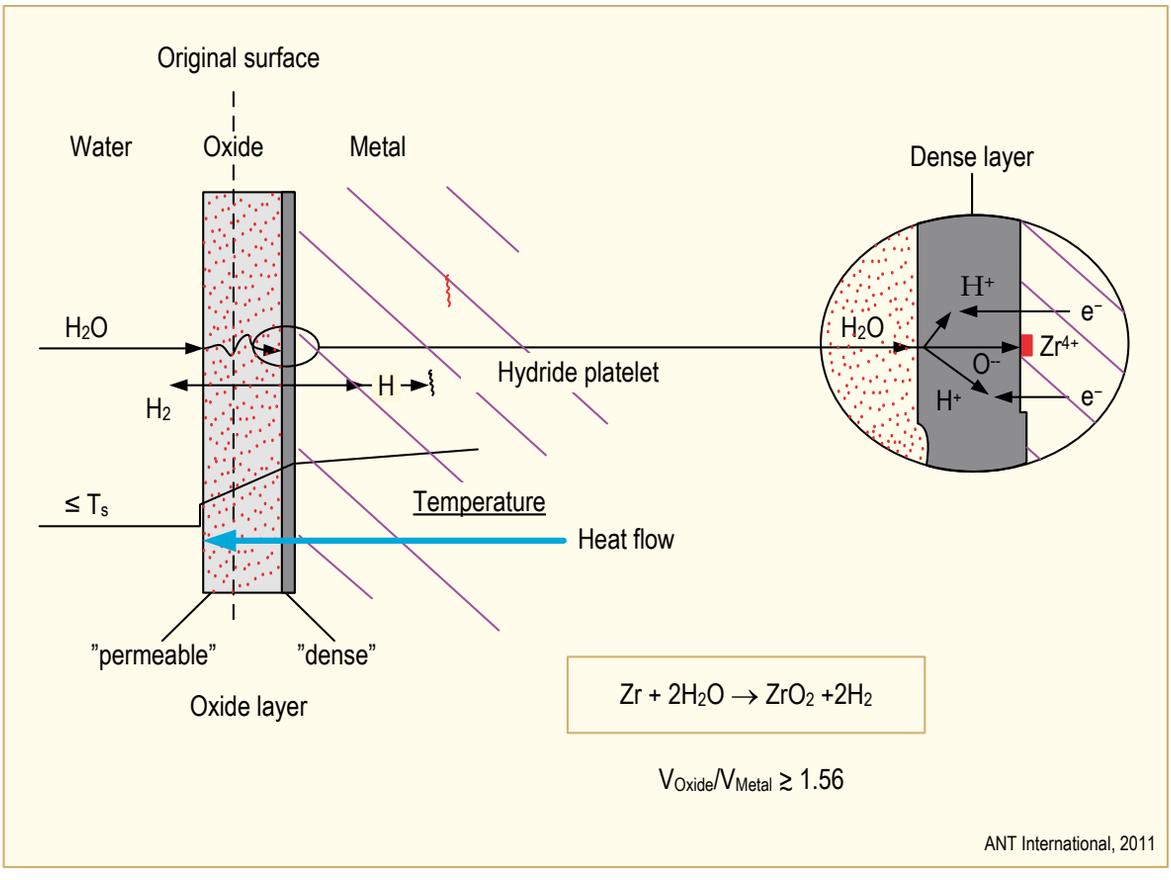

Figure 5-2: Schematic showing the corrosion and HPU process in zirconium alloys.

There are different types of corrosion modes:

- **Nodular corrosion** (almost only BWRs since it requires an oxidising environment) starting after 10 to 100 days of irradiation in material with large Zircaloy Second Phase Particles (SPPs) (Figure 5-3 and Figure 5-9). Nodular corrosion is characterized by locally a much thicker oxide patches appearing as white spots. The corrosion rate is initially very large but levels of at high burnups. Due to the low oxidation potential in a PWR/VVER only uniform corrosion normally exists (Figure 5-9). However, if for some reason there would be an increase in the coolant oxidation potential, nodular corrosion may also occur in PWRs/VVERs.

- **Uniform corrosion** (PWRs/VVERs/CANDUs/BWRs) that starts at the beginning of irradiation at a rapid rate, slows quickly (Figure 5-3 and Figure 5-9). With increasing oxidation and hydrogen absorption (pickup) at higher burnup, the concentration of hydrogen in Zr alloys can exceed it solubility limit and precipitate as hydrides. In components with heat transfer (e.g., fuel cladding), such hydrides tend to form in regions of lowest temperature. With the heat flux typical of LWR fuel rods, precipitation in regions of low temperature can lead to relatively high concentrations at the outer metal-oxide interface, which can, in turn, increase the oxidation rate.

In PWRs, there is an increase in the oxide growth rate at about 20-30 microns because solid hydrides may form in the Zr alloy at this point, thus increasing the oxide growth rate, Figure 5-8. At oxide thicknesses of about 100 microns and a large surface heat flux, there may also be a thermal feedback effect, which then leads to a second oxidation acceleration step.

In VVERs, there is normally no acceleration of the uniform corrosion process due to the very low hydrogen pickup. The reason for the low hydrogen pickup is due both to the (normal) use of the Zr1Nb alloy E110 and different coolant chemistry.

In BWRs, the SPPs (nickel-bearing and chromium-bearing SPPs) in Zry-2 starts to dissolve already at the start of irradiation due to the fast neutron flux. Dependent upon the initial size and type/chemistry of the SPP, the dissolution rate varies. At a certain fast fluence level (corresponding to a certain burnup) the SPP has completely dissolved in the matrix, the fluence level when this complete dissolution occurs increases with increased initial SPP size. When the SPPs have totally dissolved there is a dramatic increase in HPUF from 5-10% to over 100% (which means that part of the hydrogen must also come from the radiolytic hydrogen being produced) which eventually will lead to formation of a hydride rim at the metal/oxide interface. The hydride rim corrodes faster than the Zirconium alloy which means that at this point there is a corrosion acceleration.

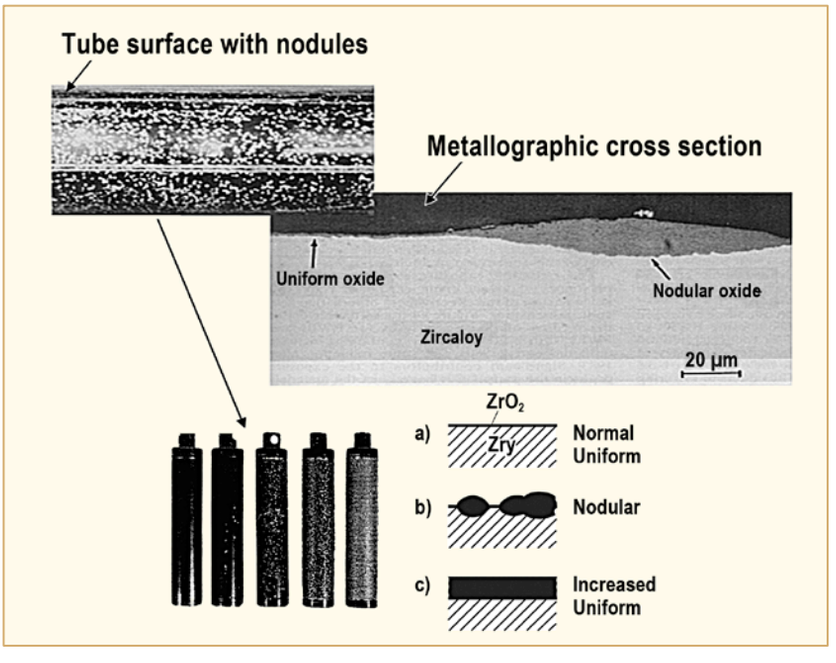

Figure 5-3: Corrosion morphology for Zircaloy [Adamson et al., 2007/2008a].

- **Shadow corrosion** (almost only in BWRs since it requires an oxidising environment) starting after a few days of irradiation (Figure 5-9), which may accelerate at higher burnups. Although agreement does not exist regarding the underlying mechanism, shadow corrosion is frequently postulated to be a galvanic type of corrosion. Shadow corrosion has "always" been present in BWRs, but not in PWRs, primarily related to the high PWR hydrogen concentration which reduces or eliminates galvanic potentials between dissimilar alloy components. Shadow corrosion occurs in areas where a Zr alloy is in contact with or in close proximity to a dissimilar material such as nickel-based alloys (Inconel) or stainless steel, e.g. spacers in case of fuel rods (Figure 5-4), and control rods in case of BWR fuel outer channels (Figure 5-5 and, Figure 5-6).

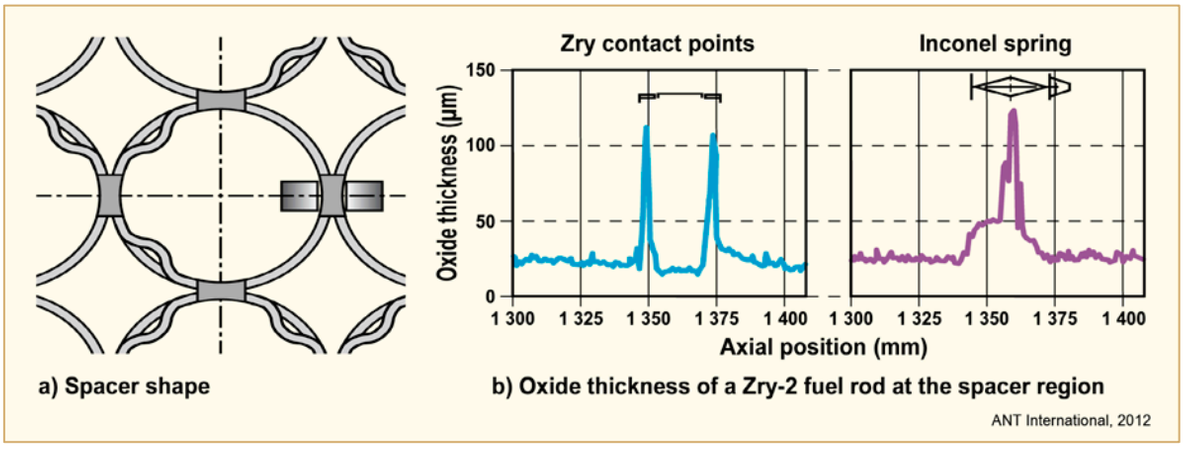

Figure 5-4: Oxide layer thickness profile of a BWR Zry-2 fuel rod opposite to Zry contact points (a) and Inconel contact point (b) after a burnup of 46 MWd/kgU, after [Garzarolli et al., 2001a].

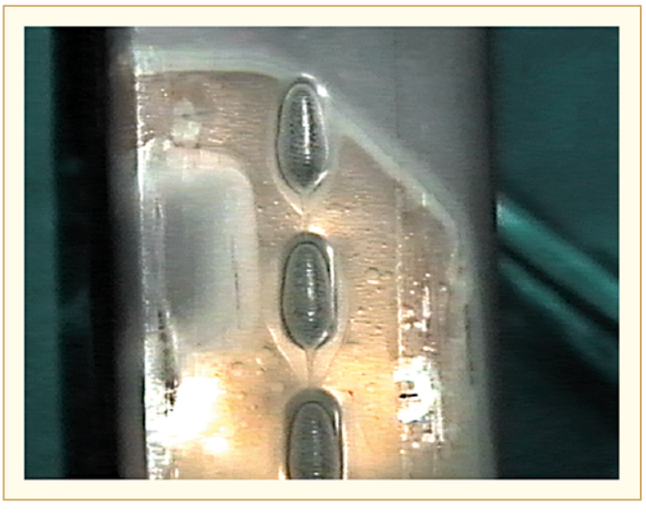

Figure 5-5: BWR channel control rod handle shadow corrosion.

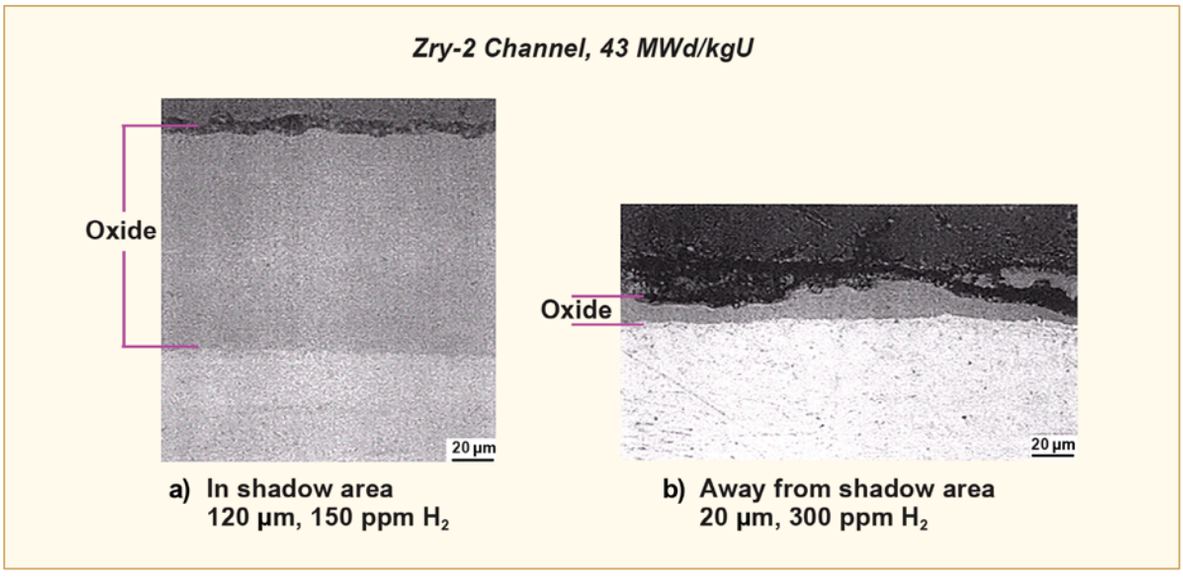

Figure 5-6: Zirconium oxides near (a) and away from (b) a stainless steel control blade bundle [Adamson et al., 2000].

There is one case when a late in life oxidation acceleration occurred; viz., Enhanced Spacer Shadow Corrosion, (ESSC)[44] in KernKraftwerk Leibstadt (KKL); see ZIRAT5/IZNA1 Annual Reports (AR) [Adamson et al., 2000/2001] for more details. The mechanism for this acceleration on oxide growth is not clear, but it may have to do with that the SPPs were dissolved at this burnup level.

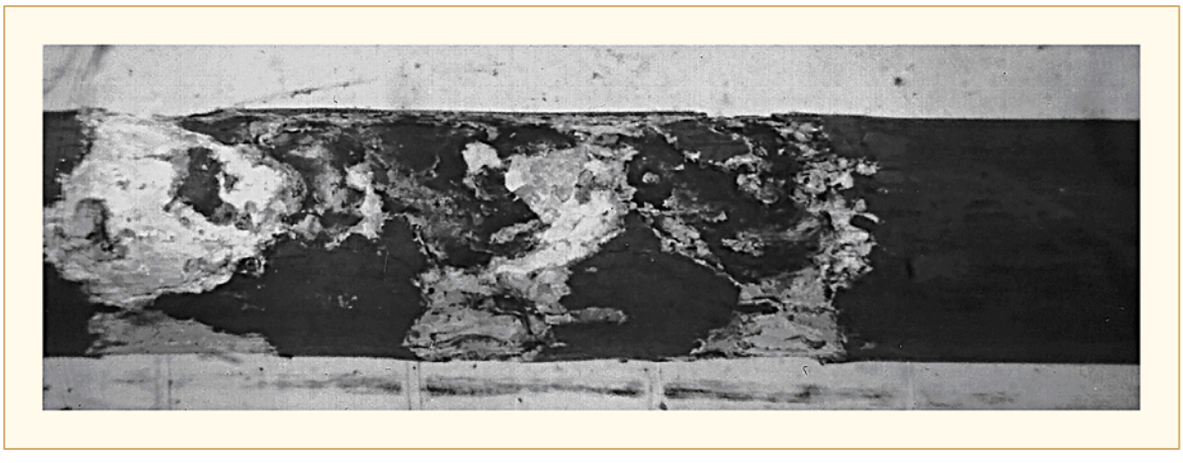

Figure 5-7: Advanced ESSC with spalling and pitting on fuel rods, shown with Inconel spacer removed [Zwicky et al., 2000].

The following figures shows the typical oxide growth in BWRs, PWRs and VVERs:

[44] This corrosion phenomenon resulted in a few failed rods. This accelerated type of corrosion occurred on the fuel cladding material at spacer locations (the spacer springs in BWR fuel assemblies are made of a Ni-alloy such as X750). Water chemistry seems also to play a role. Specifically coolant chemistry with low Fe/(Ni-Zn) ratio seems to be aggressive provided that the cladding material shows poor corrosion performance. A fuel cladding material with good corrosion resistance (i.e. larger SPPs) does not result in ESSC, enhanced spacer shadow corrosion, even in an aggressive water chemistry.

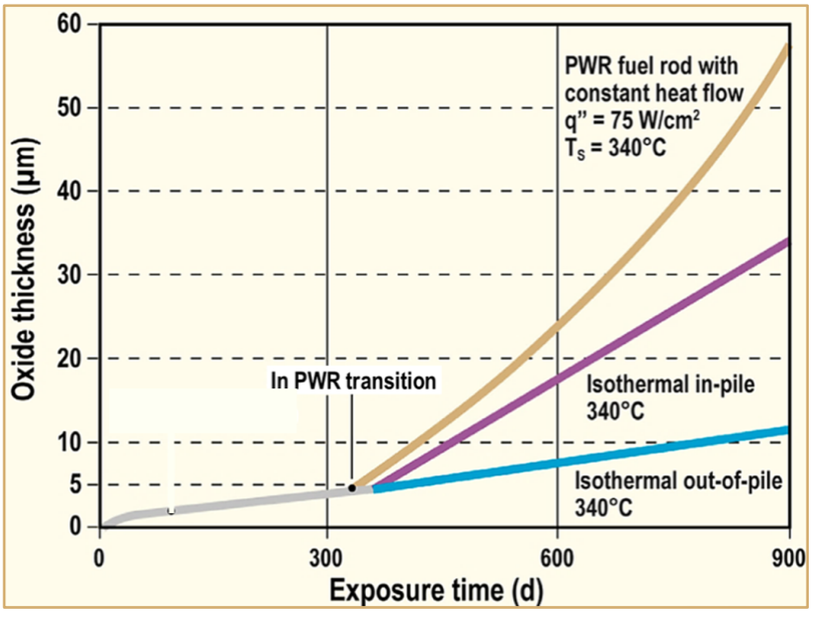

Figure 5-8: Oxide layer thickness as a function of time (schematically). Isothermal out-of-pile and in-pile, and for a fictive PWR/VVER fuel rod with constant surface heat flow [Garzarolli et al., 1985].

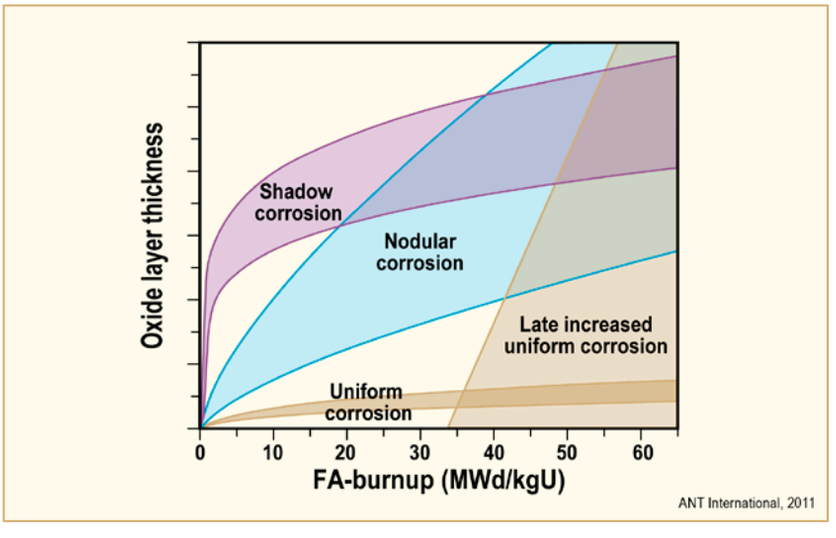

Figure 5-9: Different types of corrosion observed in BWRs. Oxide thickness is arbitrary; uniform corrosion for Zry-2 and -4 is of the order of 20-40 µm respectively for a burnup of 30 MWd/kgU.

5.1.2 Parameters impacting Corrosion and HPU

The most influential variables in the corrosion process are summarized below in the following.

5.1.2.1 Temperature

One of the most sensitive variables affecting the corrosion process is the metal-oxide interface temperature and temperature history. The factors affecting the temperature are (Figure 5-10):

- Rod power.
- Oxide thickness and its thermal conductivity.
- CRUD thickness and its thermal conductivity.

6 An introduction to Delayed Hydride Cracking (DHC) in zirconium alloys

6.1.1 Abstract

Hydrogen, in the form of hydrides, has been responsible for several failures in components made from zirconium alloys in both nuclear and chemical plants. This paper describes the mechanism of these failures caused by a time-dependent phenomenon called DHC. The most notable failures were in pressure tubes made from Zr-2.5Nb, but cracking in Zircaloy fuel cladding may also be caused by this mechanism. In DHC, hydrogen moves but hydrides crack. The requirements for the presence of hydrides are described and the range of conditions of loading and temperature history that induce cracking are reviewed. A method for safeguarding and assessing components by answering seven questions is outlined.

6.1.2 Introduction

When present in structural components, hydrides may be responsible for loss in integrity because they are brittle. In the Periodic Table the affected metals of most importance are those in Group 4 – titanium, zirconium and hafnium – and Group 5 – vanadium, niobium and tantalum [Coleman, 2003]. The damaging effect of hydrides may take the form of a reduction in short-term crack growth resistance and tensile ductility or in the form of time dependent processes. Hydrogen diffuses up stress gradients, down temperature gradients, up or down alloy solute concentration gradients and down hydrogen concentration gradients. This movement may lead to time dependent failure when the solubility limit is exceeded and hydrides form. In a water-cooled nuclear reactor, hydrogen is absorbed by a component during service as a consequence of corrosion. The hydrogen movement and increase in concentration necessitate continuous vigilance during the life of the component to ensure it performs as designed.

Time dependent cracking associated with hydrogen and hydrides was recognized as an important failure mechanism in titanium alloys in the 1950s [Kessler et al, 1955]. This failure mechanism, called **S**ustained **L**oad **C**racking (SLC), was characterized by a cracking rate, V that was highly dependent on temperature but had low dependence on load once a threshold value was exceeded. Although it turns out that zirconium alloys are much more sensitive to time-dependent hydride cracking than titanium alloys, the phenomenon became more than a laboratory curiosity in zirconium alloys only in the mid-1970s. Early indications were that zirconium alloys had high tolerance to such time dependent fracture. In tests at room temperature, notched tensile specimens of Zr-1.25Al-1Sn-1Mo in the annealed condition and containing 500 ppm hydrogen showed the characteristic behaviour of increase in time to failure as the applied stress was reduced (Figure 6-1). Specimens failed in 30 hours at about half the notched UTS, in 200 hours at 0.3 of the notched UTS, and did not fail in over 1100 hours at 0.2 of the notched UTS [Weinstein & Holtz, 1964]. Quenched and aged Zr-2.5Nb gave a slight indication of delayed failure within the limits of the test time (1000 hours), while annealed or cold-worked Zircaloy (Zr-1.5 wt.% Sn) was completely resistant. Östberg [Östberg, 1964] found some suggestion of delayed failure in Zircaloy containing 10 ppm hydrogen in tests at 100 °C.

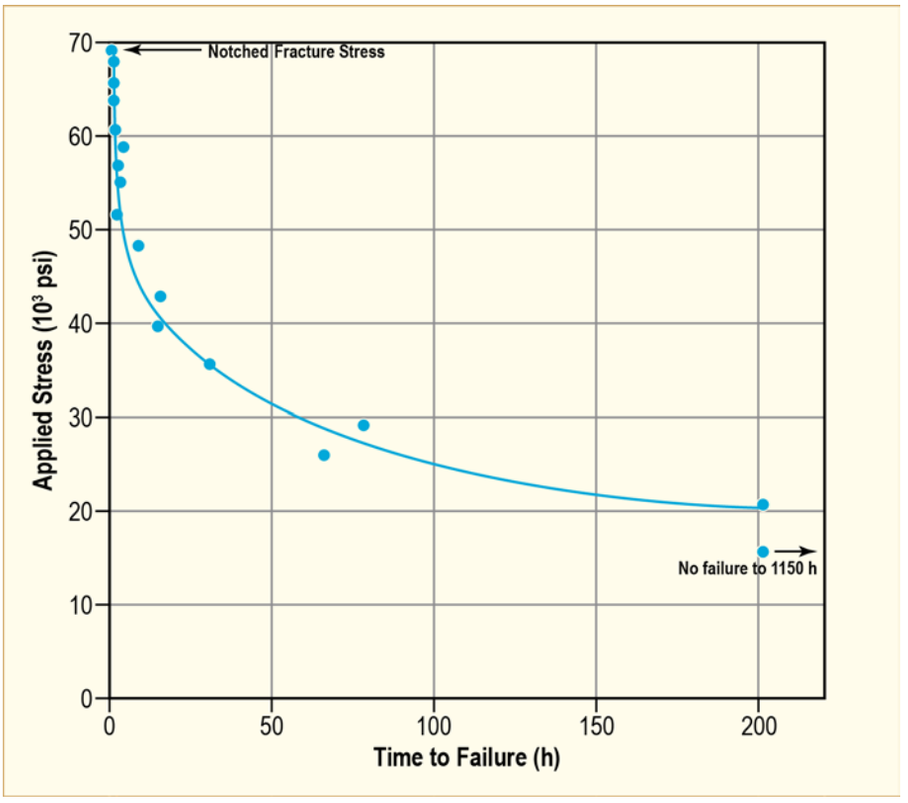

Figure 6-1: Delayed failure curve at room temperature of notched Zr-1.25Al-1Sn-1Mo specimens containing 500 ppm hydrogen [Weinstein & Holtz, 1964].

The cracking of Zr-2.5Nb pressure tubes in CANDU and Reaktor Bolshoi Mozhnosti Kanalov (in English Large Boiling Water Channel type reactor) (RBMK) reactors abruptly changed the perception on time dependent failure and generated much research into the phenomenon. The time dependent cracking in zirconium alloys has had several names but the accepted one is DHC[66]. The phenomenology is similar to that of SLC in titanium alloys. In this paper the experience with this type of cracking is outlined, the basic mechanism and phenomenology are described along with a brief presentation on the current controversy on models of crack growth rate, then the questions for assessment of structural integrity are posed.

[66] The other names that have been used in the technical literature are: delayed failure hydrogen embrittlement, delayed hydrogen embrittlement, delayed hydrogen cracking, hydrogen assisted subcritical crack growth, hydrogen-induced delayed cracking, and hydride-induced crack growth.

6.1.3 Component failure by DHC

6.1.3.1 Experience with pressure tubes

6.1.3.1.1 Pickering 3 and 4: 1974 and 1975

High residual stresses were responsible for the cracking in Zr-2.5Nb pressure tubes after two to three years of operation. In CANDU reactors, the pressure tubes are 4 mm thick, have an inside diameter of 103 mm and a length of 6 m. Each end is placed inside a thick-walled tube of 403 SS containing three internal, circumferential grooves – the end-fitting – and the pressure tube is internally rolled to make a seal at the grooves; this configuration is called a rolled-joint. If the rolls are advanced too far – called over-rolling or over-extension – part of the pressure tube is deformed without support from the SS and large residual tensile hoop stresses arise locally (Figure 6-2). A second factor is the clearance between the pressure tube and the end-fitting; the larger the clearance, the higher the residual stress. A combination of over-rolling and high clearance could produce residual stresses well over 500 MPa. Consequently, cracks may initiate. (Note that the hoop stress from the operating pressure is at least three times lower than these residual stresses.) When the cracks penetrated the pressure tube wall in 1974 (Pickering 3) and 1975 (Pickering 4), heat-transport water leaked and was detected in the gas annulus between the pressure and calandria tubes, and the reactor was shutdown. This behaviour is an example of an approach to Leak-Before-Break (LBB): detect and identify a growing and leaking but stable crack before it reaches its Critical Crack Length (CCL) and becomes unstable. Once the leaking tubes were identified, they were removed and replaced. Out of 780 tubes, eighteen in Pickering 3 and two in Pickering 4 leaked [Jackman & Dunn, 1976] and [Perryman, 1978]. Only one more leaking crack was detected after the initial set of failures.

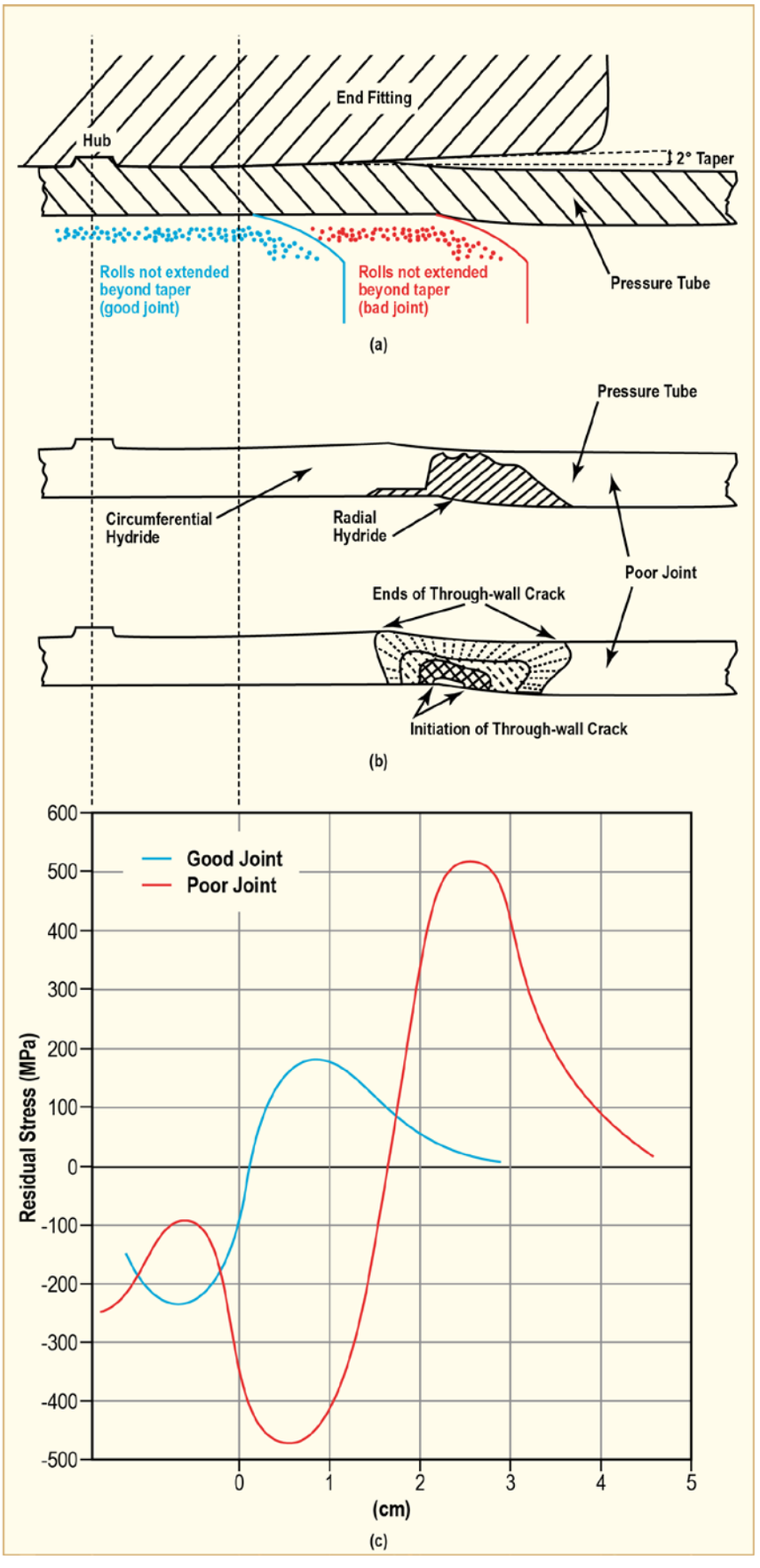

Figure 6-2: Schematic diagrams of (a) rolled-joint, (b) location of cracking and (c) residual hoop stresses for over-rolled and correctly rolled joints [Perryman, 1978].

The cracks initiated on the inside surface because the residual stresses were higher at the inside than at the outside of the pressure tube. The cracks grew radially and axially in a series of bands on a plane normal to the hoop direction with a depth-to-length ratio of about three (Figure 6-3). The fracture surfaces had the characteristics of broken hydride and hydrides were observed at the tips of surface cracks (Figure 6-4). The interpretation was that the cracks grew at low temperatures by DHC, but once the reactor was at power and the pressure tubes were at a HT, >250 °C, cracking stopped because the low hydrogen concentration, < 15 ppm, was all in solution, and the crack surfaces oxidized. Cracking continued during subsequent reactor shutdowns, and the stopped-crack continued to oxidize during power production. Each band on the fracture surface corresponded with a reactor shutdown and period of operation [Causey et al., 1977]. The crack velocities in these failures ranged from 9×10^{-11} to 5.5×10^{-10} m/s at 35 °C (about 3 to 17 mm in one year) to 7×10^{-9} m/s at 138 °C (about 4.2 mm in one week).

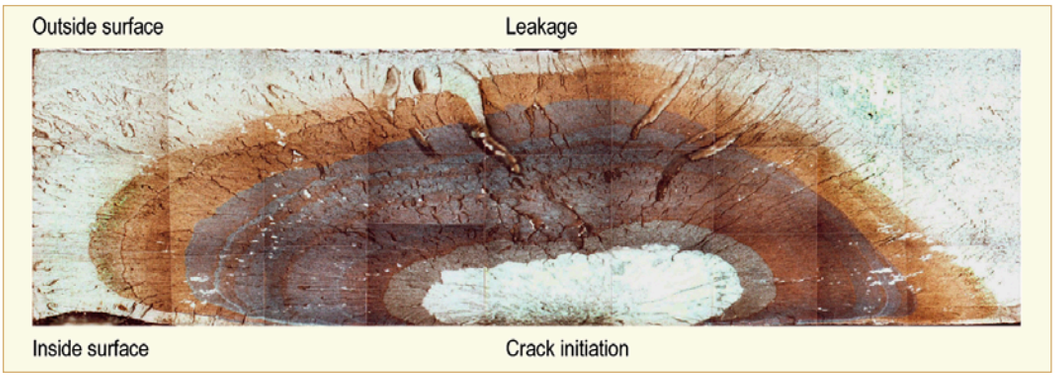

Figure 6-3: Typical crack at rolled joint in Zr-2.5Nb pressure tube [Perryman, 1978].

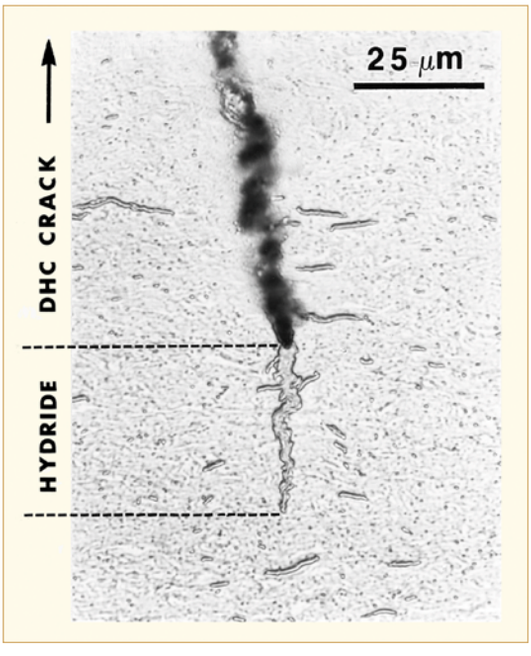

Figure 6-4: Hydride growing at end of DHC crack (photograph supplied by D.K. Rodgers).

Most of the cracking was at a specific side of the reactors (the "West" end) and at the inlet ends of the fuel channels. The reasons for these observations are:

- The "back" ends (the end of the tube that exits the extrusion press last) were placed at the west end. The grain size is smaller at the back ends so they tend to be stronger than the front ends; residual stresses would be higher with the stronger material.

- The rolled joints for the west face were installed after those for the east face. The procedures at the time allowed for more over-rolling – about 13 mm – and greater clearance between the outside of the pressure tube and inside of the end-fitting at the west face than at the east face. If the pressure tube to end-fitting clearance was greater than 0.3 mm, the residual stresses tended to be large and the probability of cracking was high.

- Across the reactor face, the inlet and outlet to the fuel channel alternate. The temperature of the heat-transport water is lower at the inlet end and the rate and amount of stress relaxation at the rolled joint from reactor operation would be smaller than at the outlet end.

Large crack initiators were absent. Small surface flaws, for example, from sand blasting, or hydride perpendicular to the tube surface were sufficient to start cracking [Cheadle & Ells, 1977]. The tubes that cracked tended to come from ingots that had high oxygen concentrations. The mean value of oxygen concentration of the tubes that cracked was 260 ppm higher than the mean concentration of the non-cracking tubes. Consequently, the tensile strength at room temperature was about 30 MPa higher [Winton & Murgatroyd, 1966] than in the non-cracking tubes, leading to larger residual stresses in these rolled joints. Since each of the above factors was distributed, pressure tubes tended to crack in rolled joints that contained all of the factors at the damaging end of their distribution, that is, west inlets with tubes containing high oxygen concentration. Rolled joints that contained none or only one or two damaging features tended not to crack, thus explaining why just a few tubes cracked and why it was not a continuous problem.

6.1.3.1.2 Bruce 2: 1982

At the time of the discovery of the cracks in the Pickering reactors, the rolled joints in the first two Bruce reactors were already made. Before these reactors went into service, the large residual stresses were removed by heat-treatment – 500 °C for 30 min. The efficacy of this heat-treatment to reduce residual hoop tensile stresses was demonstrated in a pressure tube removed from Bruce 2 before it started operating: after installation the maximum tensile stress was about 550 MPa and after heat-treatment it had been reduced to about 100 MPa [Dunn et al., 1982]. In the two years between rolling and heat-treatment, cracks had already initiated in four tubes. In Bruce 2, three tubes leaked in 1982 [Dunn & Jackman, 1982], [Cheadle et al., 1987] and one other leaked in 1986 [Rodgers et al., 1992]. The initial maximum residual tensile hoop stresses in these rolled joints were in the range 525 to 620 MPa; on removal these stresses were in the range 67 to 90 MPa, confirming that the joints had been Stress Relieved (SR). No cracking was detected in Bruce 1 because the rolled joints were made after those in Bruce 2 and the time interval between installation and stress relief was shorter in Bruce 1, providing less time for cracks to initiate.

In later reactors, the rolled joints were made with low residual stresses by minimizing the gap between the pressure tube and the end-fitting – called a zero-clearance rolled-joint – and ensuring that the rolled part of the pressure tube was firmly supported by not over-rolling. Typically the maximum residual hoop tensile stresses at the inside surface were now less than 100 MPa.

7 Zr Alloy performance during LOCA and RIA

This topic is covered more extensively in the following ANT International Reports:

- ZIRAT9/IZNA4 STR Loss of Coolant Accidents, LOCA, and Reactivity Initiated Accidents, RIA, in BWRs and PWRs [Rudling et al., 2004/2005] and,
- ZIRAT15/IZNA10 STR Processes going on in Nonfailed Rod during Accident Conditions (LOCA and RIA) [Strasser et al., 2010b].

7.1 LOCA

7.1.1 Introduction

The LOCA event starts by the decrease and then the loss of coolant flow due to a break in a coolant pipe while, at the same time, the reactor is depressurized, scrammed and shut-down. The fuel starts heating up due to its decay heat until the Emergency Core Cooling Systems (ECCSs) are activated and cools the fuel. Hypothetical LOCA events are analysed for each reactor to assure that the safety criteria, defined by the regulators, for the reactor system and the fuel, are met. The DBAs relevant to LOCA fall into two general categories. The LBLOCA, assumes a double ended break of a primary coolant cold leg of a PWR or a break in the recirculation pump intake line of a BWR either of which could cause the loss of all the coolant from the core. The small break, or Small Break LOCA (SBLOCA), assumes a break in one of the smaller primary circuit lines that will cause less coolant loss than the LBLOCA.

The effect of a LOCA cycle on the fuel is shown schematically in Figure 7-1, which plots the fuel and cladding temperatures as a function of time in the accident. The loss of coolant flow and reactor pressure at the initiation of the accident will decrease heat transfer and allow the fuel and cladding to heat up until the reactor scrams. The fuel will then cool down somewhat partly due to cooling by the steam-water mixture that is formed, but the cladding temperature will continue to rise until the reflood and quench stage.

During and after the LOCA it must be ensured that:

- The core remains coolable (which means that the maximum allowable coolant blockage is limited) and,
- No fuel dispersal occurs (which means that cladding rupture is not allowed; it is assumed that the cladding burst is so small that only fission gases are released).

Table 7-1 summarises the impact of Zr alloy properties on margins towards the LOCA design criteria.

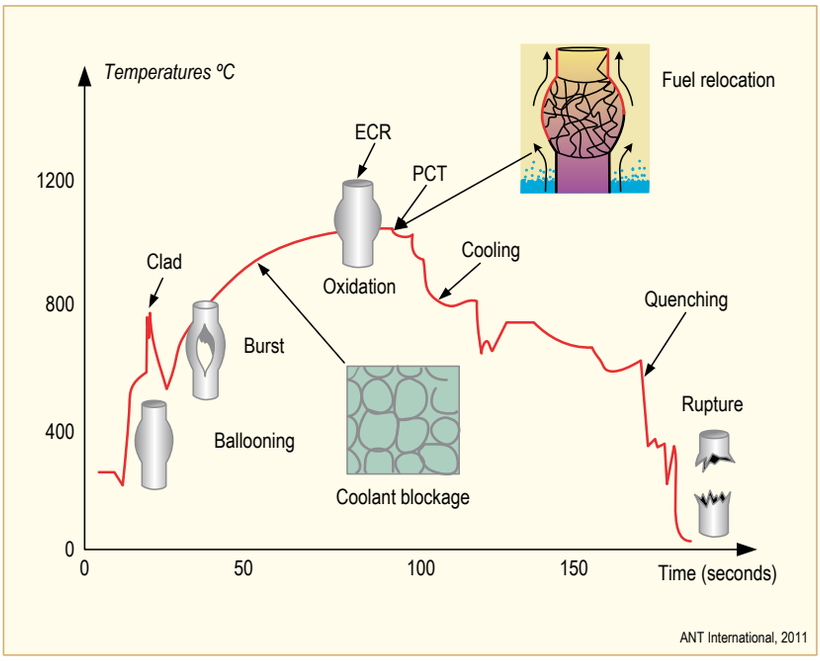

Figure 7-1: Typical LOCA in a PWR.

Table 7-1: LOCA Design Criteria and relation to Zr alloy issues and performance limitations.

Criterion	Failure mechanism	Consequences	Material parameters increasing margins to failure	Read more
LOCA – maximum 10% of the fuel rods in core may burst (Germany)	FR burst		Reduce the fuel clad hydrogen content	e.g. FDRH [Strasser et al., 2010a] and ZIRAT15/IZNA10 STR Vol. II, 2010
LOCA – retaining fuel clad ductility	Fuel cladding fracture (and fuel dispersal)	Non-coolable fuel geometry	Increase fuel clad ductility by: 1) reducing hydrogen clad pickup from pre-LOCA irradiation as well as during LOCA HT oxidation, 2) reduce the HT LOCA clad oxidation	e.g. FDRH [Strasser et al., 2010a] and ZIRAT15/IZNA10 STR Vol. II, 2010
				© ANT International 2011

In the following subsections, the effects of Zr alloy properties on LOCA fuel performance are described.

The fuel cladding material impacts: 1) creep and burst behaviour, 2) oxidation correlation, 3) margin towards breakaway oxidation and 4) post quenched ducility. All these parameters are covered in the following.

7.1.1.1 Ballooning

The loss of coolant flow decreases heat transfer from the fuel, increases the fuel temperature and causes a significant temperature rise of the cladding. The decrease in system pressure causes a pressure drop across and a hoop stress in the cladding. The result is the creep deformation, or ballooning of the cladding. Depending on the temperature, the cladding ductility and the rod internal pressure, the cladding will either stay intact or burst. Ballooning of the FRs may result in blockage of the coolant sub-channels that in turn may impact the fuel coolability. If large fuel clad burst strains occur at the

same axial elevation leading to co-planar deformation in or among FAs, coolability may be significantly degraded. The extent of the ballooning is dependent on:

- Creep strength of the cladding which depends on:
  - Alloy composition
  - Fuel clad hydrogen content (picked up during the water-zirconium alloy corrosion reaction during reactor operation prior to LOCA), see Figure 7-2 and Figure 7-3
  - Microstructure
  - Texture
  - Oxidation during the LOCA

The elevated LOCA temperatures will anneal radiation damage and any CW remaining from the fabrication process

- Stress and corresponding strain rate the cladding is subjected to,
- Temperature and the rate of temperature rise assumed for the DBA.

Figure 7-2 shows that hydrogen decreases the α/α+β phase transformation temperature, which means that increasing the hydrogen content in the fuel cladding will lower its ductility and result in more FR ruptures during a LOCA. Figure 7-3 shows that fuel clad ductility in thermal creep tests is lower for prehydrided[69] Zry-4 than that of Zry-4 with low hydrogen content.

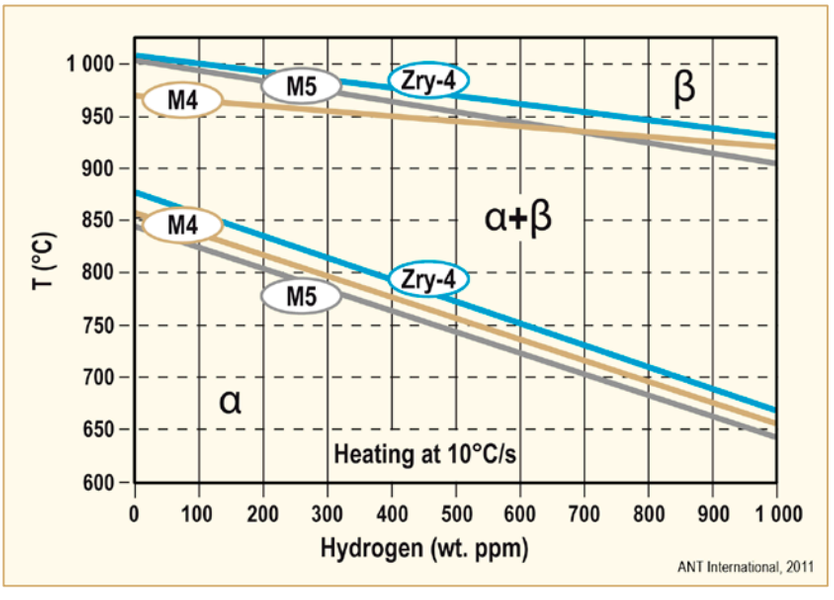

Figure 7-2: Scheme of the α/β phase transformation temperatures of Zry-4, M4 and M5 alloys as a function of the hydrogen content for an heating rate of 10°C/s (18°F/s), after [Brachet et al., 2002].

[69] Prehydriding is being done to simulate the HPU during the base irradiation prior to the hypothetical LOCA event.

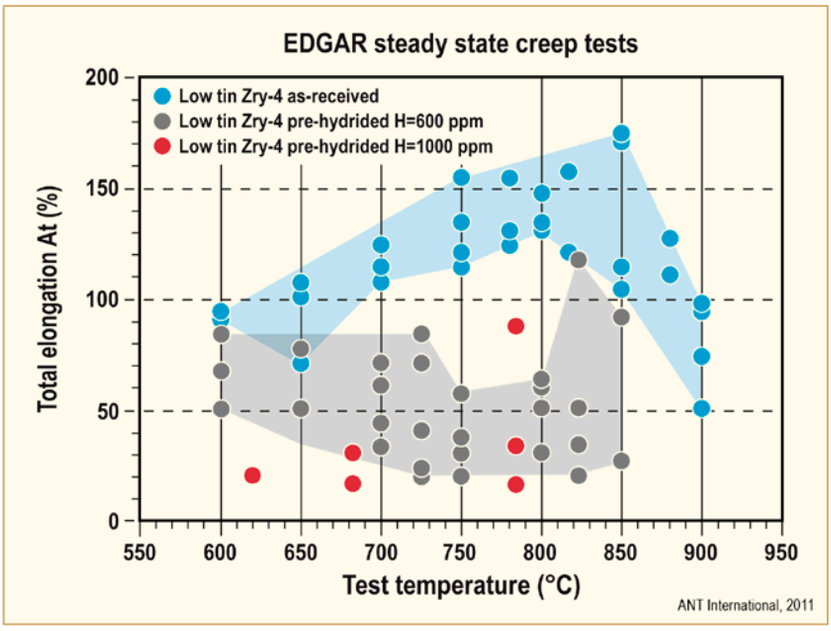

Figure 7-3: Isothermal creep tests results of unirradiated Zry-4, after [Waeckel & Mardon, 2004].

7.1.1.2 Oxidation

The increasing temperatures and presence of steam will cause the intact cladding to oxidize on the OD[70] and the burst cladding to oxidize on both the O+D and ID (two sided oxidation). The oxidation process at the high LOCA temperatures will increase the oxygen and hydrogen content in the cladding, reducing its ductility and resistance to rupture. Two sided oxidation can have significant effects on the Post Quench Ductility (PQD) of the cladding as a result of high, but localized HPU in addition to the oxidation.

During a LOCA, fuel cladding continues to oxidize until the ECCS becomes effective and a Peak Cladding Temperature (PCT) is reached. The maximum PCT is regulated to be 2200°F by the United States Nuclear Regulatory Commission (USNRC) and 1200°C internationally.

The length of time at the PCT is determined by the reactor system and regulated by the Equivalent Clad Reacted (ECR) limit, defined as the total thickness of cladding that would be converted to stoichiometric ZrO_2 from all the oxygen contained in the fuel cladding as ZrO_2 and oxygen in solid solution in the remaining metal phase. The USNRCs ECR limit at this time is 17%. In the past, ECR was calculated by the Baker-Just (B-J) equation. ECR calculations in the US have been changed to the Pawel-Cathcart equation by the NRC. Current regulations require that ballooning and rupture be calculated for double sided oxidation and that pre-LOCA oxidation should be subtracted from the 17% total limit.

The oxide formed during the oxidation period is adherent and protective. However, after an extended period of time, generally beyond the typical LOCA cycle time, breakaway oxidation may occur when the protective oxide film cracks and exposes fresh cladding surface to the oxidizing atmosphere. *The change in oxide film characteristics are accompanied by a change from parabolic to quasi-linear oxidation kinetics, a process that will accelerate the HPU during the HT oxidation and thereby further embrittle the cladding and reduce the PQD (***Error! Reference source not found.**). Historically, the potential of *breakaway oxidation* during a LOCA has never been in question for western alloys, since breakaway occurs at >3000 seconds at PCT compared to the LOCA cycle time of about 200 seconds. However, tests of the Russian E110 alloy revealed breakaway corrosion in <1000 seconds. Subsequent

[70] Regulatory bodies are also currently considering ID oxidation of intact cladding via transfer of oxygen from the fuel pellets.

research indicated that the shorter time to breakaway corrosion in E110 was due to fabrication related factors. Tests also showed the time to breakaway oxidation is extended to that of western alloys if E110 is made from Kroll process zirconium sponge instead of the Russian electrolytic/iodide process and if the surface finish is improved by belt sanding instead of the Russian pickling process. As an outgrowth of the E110 experience, the proposed current NRC regulations require periodic qualification testing to demonstrate that all alloys meet a minimum time to breakaway corrosion.

7.1.1.3 Cooling, quenching and embrittlement

Activation of the ECCS will stop the temperature rise and start cooling the core by injection from the bottom of the core in a PWR. The "cooling" process as shown on Figure 7-1 is relatively slow until the emergency coolant contacts the fuel that has been at the PCT. At that point, in the range of 400° to 800°C, identified as "quenching" in Figure 7-1, the water from the ECCS will reduce the cladding temperature at a rapid rate (1°–5°C/sec) by re-wetting the cladding heat transfer surface. The process will collapse the vapour film on the cladding OD and cooling will be by nucleate boiling. Thermal shock due to the sudden change in heat transfer conditions can fracture the cladding at this stage. The ability of the cladding to withstand the thermal stresses will depend on the extent of oxidation and degree of cladding embrittlement that occurred during the LOCA transient.

The oxidation embrittlement process and final structure of the cladding after completion of the LOCA cycle is shown on Figure 7-4. The overall process is as follows:

- First, the increasing water and steam temperatures during heat-up increase the reaction rates with the cladding and increase the conversion of the cladding surface into thicker ZrO_2 films.
- As the LOCA temperature passes the levels where $\alpha \rightarrow \beta$transformations start and finish, shown in Figure 7-2 for Zry-4 and M5, the resulting structure consists of:
  - The growing ZrO_2 layer,
  - a zirconium alloy layer with a very high oxygen content which stabilizes the α phase,
  - the bulk cladding which is now in the β phase.
- The ECCS initiated quenching phase cools the cladding back down through the$\beta \rightarrow \alpha$ transformation temperature and the bulk cladding is now re-transformed from the β into the α phase, which is referred to as the "prior or former β phase".

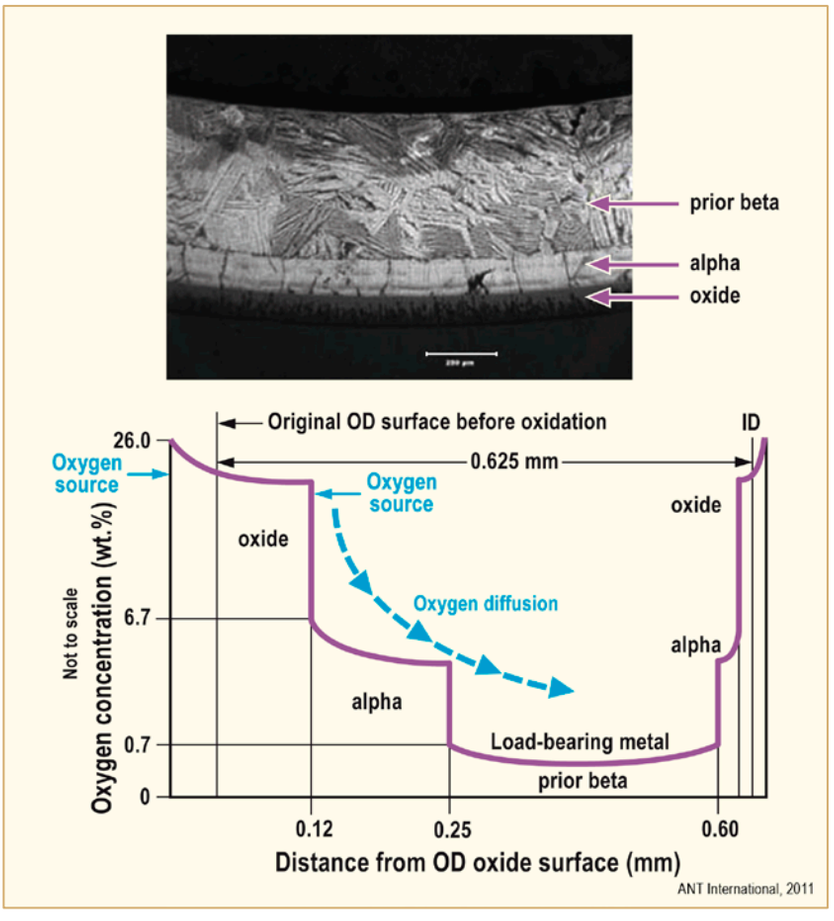

Figure 7-4: Structure of oxidized cladding, after [Meyer, 2005]. (The presence of Nb would result in a similar structure except the boundary between the alpha and the prior beta phase would be more uneven).

Oxygen and hydrogen affect the formation of the structure as follows during the oxidation:

- Oxygen diffuses from the ZrO_2 to the bulk cladding which is in the β phase at HT; however, the β phase has a low solubility for oxygen.
- *Increased hydrogen levels from the oxidation reactions prior to and during the LOCA increase the diffusion rate and solubility of oxygen in the β phase at temperatures >1000°C.*
- Wherever the solubility limit of oxygen in the β phase is exceeded, the excess oxygen stabilizes the α phase.
- The oxygen stabilized α phase forms next to the ZrO_2 layer. Both the stabilized α phase and the ZrO_2 layer grow at the expense of the bulk cladding in the β phase. due to HTPs and as a result of quenching in the "prior β phase".

The final integrity of the cladding is based on the properties of the prior β phase, since the ZrO_2 and oxygen stabilized α zones are too brittle to sustain a load.

Again, it is important to note that variables assumed for cooling and quenching during the DBA will have a significant effect on the degree of embrittlement and the PQD:

- Slow cooling rates from the PCT to the quenching temperature will increase the PQD.
- Lower quenching temperatures, such as 600°C instead of 800°C, will increase the PQD.
- Lower quenching rates from the quenching temperature will also increase the PQD.

8 Interim dry storage

8.1 Introduction

As of mid-2010, about 225 000 tons of Spent Nuclear Fuel (SNF) wasstored around the worldunder either wet or dry conditions in pools (ponds) and dry storage facilities [Sokolov, 2010]. To-date, experience with SNF storage has been free of major incidents. Storage is only an interim, temporary step in the overall fuel cycle: SNFcan be classified as a resource to be eventually re-used or as a waste to be disposed of in a geologic repository. The "resource vs. waste" classificationis often a matter of national policy, which can be periodically re-assessed as national interests and energy market conditions evolve.

Except for fuel rods that failed during in-reactor operations, fuel cladding integrity is a key operational and regulatory concern during SNF storage and transportation. Similarly, fuel assemblies (FAs) are structural entities that enable handling, loading, and retrieval from storage systems. Under normal storage and transportation conditions, fuel rods are generally expected to maintain their integrity and FAs are required to maintain their geometric configuration. Under hypothetical accident conditions, regulations related to sub-criticality, shielding (external surface radiation level limits) and effectiveness of packaging in limiting releases of radionuclidesmust be satisfied; in order to do so, credible assessments of the structural performance of fuel rodsand FAs may be required.

8.2 Degradation Mechanisms

Potential degradation mechanisms that may affect cladding integrity of SNF during dry storage and transportation operations are:

- Air oxidation;
- Thermal creep;
- Stress corrosion cracking (SCC);
- Delayed hydride cracking (DHC);
- Hydride reorientation;
- Hydrogen migration and redistribution.

The first mechanism is of specific interest when considering loss of inerting conditions when the inert gas (typically He) is replaced by air. The next three mechanisms have the potential to result in through-wall cladding defects during storage. The last two are unlikely to result in fuel rod failure during storage; rather, they have the potential to impact the ability of the cladding to withstand adverse mechanical challenges from handling or transportation accidents.

For more detailed discussions of these mechanisms, see for examples: [IAEA, 2012b] and [Patterson C. and F. Garzarolli, 2015].

8.2.1 Air oxidation of cladding

Because oxidation rates of zirconium-based cladding by air are relatively low at temperatures typical of dry storage conditions, losses in cladding wall thickness are limited to a few percent, even after prolonged air exposure.[75] Therefore, cladding remains an effective containment barrier protecting the fuel pellets from exposure to air for fuel rods that do not contain through-wall defects.

[75] See for example, [Hillner E., D.G. Franklin, and J.D. Smee, *The Corrosion of Zircaloy Clad Fuel Assemblies in a Geologic Repository Environment,* WAPD-T3173. 1998]. The Hillner et al.'s equation was developed for steam corrosion, but the corrosion rates in steam and air are similar.

References

10 CFR Part 50 Appendix A, *General Design Criteria for Nuclear Power Plants*, US, Government Printing Office, Washington, 1990.

10 CFR Part 100, NRC, Standard Review Plan, NUREG-0800, USNRC, 1995.

Adamson R. B., *Irradiation Growth of Zircaloy*, Zirconium in the Nuclear Industry; Third Conference, ASTM STP 633, pp. 326, 1977.

Adamson R. B., *Effects of Neutron Irradiation on Microstructure and Properties of Zircaloy*, Zirconium in the Nuclear Industry; 12th International Symposium, ASTM STP 1354, pp. 15-31, West Conshohocken, PA, 2000.

Adamson R. B., Lutz D. R. and Davies J. H., *Hot Cell Observations of Shadow Corrosion Phenomena*, Proceedings Fachtagung der KTG-Fachgruppe, Brennelemente und Kernbautelle, 29 Februar/1 Marz 2000, Forschungszentrum Karlsruhe, 2000.

Adamson R. B. and Rudling P., *Mechanical Properties of Zirconium Alloys*, ZIRAT6/IZNA1 Special Topics Report, ANT International, Mölnlycke, Sweden, 2001/2002.

Adamson R. et al., *The Annual Review of Zirconium Alloy Technology for 2000*, ZIRAT5/IZNA1 Annual Report, ANT International, Mölnlycke, Sweden, 2000/2001.

Adamson R. B. and Rudling P., *Dimensional Stability of Zirconium Alloys*, ZIRAT7/IZNA2 Special Topics Report, ANT International, Mölnlycke, Sweden, ANT International, 2002/2003.

Adamson R. B. et al., *Corrosion of Zirconium Alloys*, ZIRAT7/IZNA2 Special Topics Report, ANT International, Mölnlycke, Sweden, 2002/2003.

Adamson R. B. et al., *High Burnup Fuel Issues*, ZIRAT8/IZNA3 Special Topic Report, ANT International, Mölnlycke, Sweden, 2003/2004.

Adamson R. B. and Cox B., *Impact of Irradiation on Material Performance*, ZIRAT10/IZNA5 Special Topics Report, ANT International, Mölnlycke, Sweden, 2005/2006.

Adamson R. et al., *Pellet-Cladding Interaction (PCI and PCMI)*, ZIRAT11/IZNA6, Special Topics Report, ANT International, Mölnlycke, Sweden, 2006/2007.

Adamson R. et al., *Corrosion Mechanisms in Zirconium Alloys*, ZIRAT12/IZNA7 Special Topics Report, ANT International, Mölnlycke, Sweden, 2007/2008a.

Adamson R. et al., *ZIRAT12/IZNA7 Annual Report*, ANT International, Mölnlycke, Sweden, 2007/2008b.

Adamson R. B. et al., *ZIRAT14/IZNA9 Annual Report*, ANT International, Mölnlycke, Sweden, 2009a.

Adamson R. B. et al., *ZIRAT15/IZNA10 Annual Report*, ANT International, Mölnlycke, Sweden, 2010.

Adamson R. et al., *ZIRAT16/IZNA11 Annual Report*, ANT International, Mölnlycke, Sweden, 2011.

Adamson R. et al., ZIRAT16 Annual Report, Advanced Nuclear Technology International, Mölnlycke, Sweden, 2011.

Adamson R., Coleman K., Mahmood T., Rudling P., *Mechanical Testing of Zirconium Alloys Volume I*, ZIRAT18/IZNA13, Special Topics Report, ANT International, Mölnlycke, Sweden, 2013.

Adamson R. B., Coleman K., Mahmood S. T., Rudling P., *Mechanical Testing of Zirconium alloys,* ZIRAT18/IZNA13 Special Topic Report, Vols. I and II, Advanced Nuclear Technology International, Mölnlycke, Sweden, 2013/2014.

Adamson R. et al., *Irradiation Growth of Zirconium Alloys - A Review*, Advanced Nuclear Technology International, Mölnlycke, Sweden, 2017

Aleshin Y. and Sparrow J., *WEC Design Experience to Reduce IRI Potential in Susceptible Cores*, JahrestagungKerntechnik, Dresden, 2009.

Alvarez Holston A-M. et al., *A Combined Approach to Predict the Sensitivity of Fuel Cladding to Hydrogen-Induced Failures during Power Ramps*, Proceedings of 2010 LWR Fuel Performance/Top Fuel/WRFPM, Paper 127, Orlando, Florida, USA, September 26-29, 2010.

Ambler J. F. R. and Coleman C. E., *Acoustic Emission During Delayed Hydrogen Cracking in Zr-2.5 wt% Nb alloy*, Proc. Second International Congress on Hydrogen in Metals), Paper 3C10, Pergamon Press, Oxford, 1977.

Ambler J. F. R., *Effect of Direction of Approach to Temperature on the Delayed Hydrogen Cracking Behaviour of Cold-worked Zr-2.5Nb*, Zirconium in the Nuclear Industry – 6th International Symposium, ASTM STP 824, D. G. Franklin and R. B. Adamson, Eds., American Society for Testing and Materials), 653-674, Philadelphia, PA, 1984.

Amouzouvi K. F. and Clegg L. J., *Effect of Heat Treatment on Delayed Hydride Cracking in Zr-2.5 wt pct Nb*, Met. Trans. A., 18A), 1687-1694, 1987.

Andersson B., *The Enhanced Spacer Shadow Corrosion Phenomenon*, Fachtagung der KTG-FachgruppeBrennelemente und Kernbauteile, 29 February/1 March 2000, Forschungszentrum Karlsruhe, 2000.

Andresen P. L., Ford F. P., Murphy S. M., Perks J. M., *State of Knowledge of Radiation Effects on Environmental Cracking in Light Water Reactor Core Materials*, pp. 1-83 to 1-121, Proceedings of the 4th Conference on Environmental Degradation of Materials in Nuclear Power Systems – Water Reactors, Jeckyll Island, GA, August 1989, (NACE, Houston, 1990).

Andresen P. L., *Stress Corrosion Cracking – Material Performance and Evaluation*, Ed. R. H. Jones ASM, p. 181, 1992.

Andriambololona H. et al., *Methodology for a Numerical Simulation of an Insertion or a Drop of the Rod Cluster Control Assembly in a PWR*, Nuclear Engineering and Design 237, 600–606, 2007.

Anon, *The Boiler and Pressure Vessel Code, American Society of Mechanical Engineers*, Section VIII, Division I, Subsection C, UNF-56, (d), p. 183, 1992.

Anon, Canadian Standards Association, *Technical Requirements for In-service Evaluation of Zirconium alloy Pressure Tubes in CANDU Reactors*, N285.8-05, 2005.

ANS, *American National Standard for Light Water Reactors, Fuel Assembly Mechanical Design and Evaluation*. 1981.

Aomi M. et al., *Evaluation of Hydride Reorientation Behaviour and Mechanical Properties for High-Burnup Fuel-Cladding Tubes in Interim Dry Storage*, Journal of ASTM International, Vol. 5, No. 9, JAI101262,2008.

Arborelius J. et al., *Advanced Doped UO_2 Pellets in LWR Applications*, Water Reactor Fuel Performance Meeting, Kyoto, Japan, Japanese Nuclear Society, 2005.

Armijo, J.S., Coffin L. F. and Rosenbaum,H.S., *Development of Zirconium-Barrier Fuel Cladding*, Zirconium in the Nuclear Industry., 10th International Symposium, ASTM STP 1245, Garde A.M., Bradley E.R., (Eds.), American Society for Testing and Materials, West Conshohocken, PA, pp. 3-18, 1994.

Armijo J. S., *Performance of Failed BWR Fuel*, Proceeding from Light-Water-Reactor-Fuel-Performance, pp. 410-422, West Palm Beach, FL, April 17-21, 1994.

ASME, *Boiler and Pressure Vessel Code, Section III - Rules for Construction of Nuclear Power Plant Components: Division 1*. New York, New York, USA, American Society of Mechanical Engineers, 2015.

Aulló M and Rabenstein W. D., *European Fuel Group Experience on Control Rod Insertion and Grid to Rod Fretting*, IAEA TC Meeting on Fuel Assembly Structural Behaviour, Cadarache - November 2004.

Aulló M., Garcia-Infanta J. and Chapin D., *Post Irradiation Examination of High Burnup Assemblies in Vandellos II*, LWR Fuel Performance Conference, Orlando, Florida, September, 2010.

Aulló M., Aleshin Y. and Messier J., *Reduction of Fuel Assembly Bow with the RFA Fuel*, Top Fuel, 2012.

Averin S. A. et al., *Evolution of Dislocation and Precipitate Structure in Zr alloys Under Long Term Irradiation*, Zirconium in the Nuclear Industry: 12th International Symposium, ASTM STP 1354, G. P. Sabol and G. D. Moan, Eds., American Society for Testing and Material, pp. 105-121, West Conshohocken, PA, 2000.

B&W-Report, *Mk-B Mechanical Design Report*, BAW-10172NP, 1989.

Bales M. and Clifford P., *Proposed Changes in Regulation for LOCA and RIA in the US*, Fuel Safety Research Meeting, Mito, Japan, October 18–19, 2016.

Barberis P. et al., CASTA DIVTM: *Experiments and Modelling of Oxide Induced Deformation in Nuclear Components*, 15th ASTM International Symposium: Zirconium in the Nuclear Industry, Sun River, OR, June 2007.

Barraclough K. G., and Beevers C. J., *Some Observations on Deformation Characteristics of Bulk Polycrystalline Zirconium Hydride: Part 1 The Deformation and Fracture of Hydrides Based on the Delta Phase*, J. Materials Science, 4, pp. 518-525, 1969.

Beck R. and Mueller W., *Mechanical Properties of Solid Zirconium Hydride*, Nuclear Metallurgy: A Symposium on Metallic Moderators and Cladding Materials, Vol. VII, p. 65, AIMMPE, New York, Oct. 1960.

Bieli R. et al., *Abnormal Bow of Zircaloy-2 Fuel Channels Without Shadow Corrosion Influence*, Jahrestagung, Germany, 2011.

Billaux M. R., Van Swam L. F. and Shann S–H., *Effect of Grain Size on the Fission Gas Release from the Rim of High Burnup Fuel Pellets*, ANS Topical Meeting on Light Water Reactor Fuel Performance, West Palm Beach, Florida, April 17-21, 1994.

Billone M.C., Yan Y., Burtseva T.A., Meyer R.O., *Cladding Behavior During Postulated Loss-of-Coolant Accidents*", USNRC Report NUREG/CR-7219, ANL-16/09, 2016

Björnkvist L. and Kee E., *Application of a Semi-empirical Rod Drop Model for Studying Rod Insertion Anomalies at South Texas Project and Ringhals Unit 4*, 1997 Int. Topical Meeting on Light Water Reactor Fuel Performance, Portland, Oregon, March 2-6, 1997.

Blat-Yrieix M. et al., *Toward a Better Understanding of Dimensional Changes in Zircaloy-4: What is the Impact Induced by Hydrides and Oxide layer?*, Journal of ASTM International, Vol. 5, No. 9, Paper ID JAI101321, 2008.

Blavius D., Mueuch E-J. and Garner N. L., *Dimensional Behaviour of Fuel Channels – Recent Experience and Consequences*, ANS/TOPFUEL, San Francisco, October, 2007.

Böke H., *Approaches to Analyze the Bowing of German PWR Fuel Assemblies*, Annual Meeting on Nuclear Technology, Stuttgart, 2012.

Unit conversion

TEMPERATURE		
°C + 273.15 = K	°C × 1.8 + 32 = °F	
T(K)	T(°C)	T(°F)
273	**0**	32
289	16	61
298	25	77
373	**100**	212
473	**200**	392
573	**300**	572
633	360	680
673	**400**	752
773	**500**	932
783	510	950
793	520	968
823	550	1022
833	560	1040
873	**600**	1112
878	605	1121
893	620	1148
923	650	1202
973	**700**	1292
1023	750	1382
1053	780	1436
1073	**800**	1472
1136	863	1585
1143	870	1598
1173	**900**	1652
1273	**1000**	1832
1343	1070	1958
1478	1204	**2200**

Radioactivity	
1 Sv	= 100 Rem
1 Ci	= 3.7×10^{10} Bq = 37 GBq
1 Bq	= 1 s^{-1}

MASS	
kg	lbs
0.454	**1**
1	2.20

DISTANCE	
x (µm)	x (mils)
0.6	0.02
1	0.04
5	0.20
10	0.39
20	0.79
25	0.98
25.4	**1.00**
100	3.94

PRESSURE		
bar	MPa	psi
1	0.1	14
10	**1**	142
70	7	995
70.4	7.04	**1000**
100	10	1421
130	13	1847
155	15.5	2203
704	70.4	**10000**
1000	100	14211

STRESS INTENSITY FACTOR	
MPa√m	ksi√inch
0.91	**1**
1	1.10